Università degli Studi di Padova

Dipartimento di Scienze Cardiologiche, Toraciche e Vascolari

CORSO DI DOTTORATO DI RICERCA IN: SCIENZE MEDICHE, CLINICHE E SPERIMENTALI

CURRICOLO: METODOLOGIA CLINICA, SCIENZE ENDOCRINOLOGICHE, DIABETOLOGICHE E NEFROLOGICHE

CICLO XXIX

STUDY OF THE CONTRIBUTION OF MUSCLE INFLAMMATION, IMAT ORIGIN AND MICROENVIRONMENT TO SARCOPENIC OBESITY

Tesi redatta con il contributo finanziario della Fondazione Cariparo

Coordinatore: Ch.mo Prof. Gaetano Thiene

Supervisore: Ch.mo Prof. Roberto Vettor

Dottoranda : Giovanna Spiro

CONTENTS

RIASSUNTO

Introduzione

La condizione ottimale attraverso cui il muscolo scheletrico può espletare la propria funzione è rappresentata da un' efficiente attivazione dei processi che regolano lo sviluppo, la crescita, la rigenerazione e il metabolismo del muscolo stesso. Quando viene a mancare l'equilibrio tra questi eventi è il momento in cui insorge una condizione patologica. Nello specifico, una perdita o riduzione di massa e funzionalità muscolare è collegata a gravi malattie, quali distrofie, cancro, obesità e processi di invecchiamento.

In questo contesto, l'obesità sarcopenica, una malattia metabolica che porta ad atrofia delle fibre muscolari e riduzione delle cellule staminali (chiamate nel muscolo cellule satelliti), è associata ad un aumento in zone ectopiche di tessuto adiposo, a riduzione della tolleranza al glucosio e a perdita di forza e motilità soprattutto in adulti e anziani.

Questo accumulo di acidi grassi in altri distretti corporei, compreso il muscolo scheletrico, induce disfunzioni metaboliche, alterazioni nella β-ossidazione, aumento di produzione di ROS, lipotossicità e insulino-resistenza. Inoltre questo tessuto adiposo intermuscolare (IMAT) agisce come chemoattrattivo per le cellule infiammatorie, soprattutto macrofagi, che, una volta in sede, producono elevate quantità di citochine pro-infiammatorie (TNF-α, IL-6, IL-1, INFγ) e basse quantità di citochine anti-infiammatorie (IL-4, IL-10). Tutto ciò porta ad un costante basso grado di infiammazione sistemica e a conseguente perdita di massa muscolare.

Scopo

Scopo di questo lavoro è quello di investigare l'origine del tessuto adiposo intermuscolare e i meccanismi che regolano il dialogo tra questo e il tessuto muscolare circostante.

La prima parte dello studio ha lo scopo di capire, utilizzando biopsie muscolari, le differenze che ci sono a livello di infiammazione del muscolo in soggetti obesi normoglicemici e diabetici rispetto ai pazienti sani. Inoltre, analizzando i sieri di pazienti che appartengono alle stesse categorie

sopraelencate, saranno individuati possibili miRNA da utilizzare come marcatori identificativi delle alterazioni muscolari in presenza di obesità.
Poiché in malattie croniche, quali obesità e diabete di tipo2, diversi fattori contribuiscono alla patologia, abbiamo deciso di investigare anche il microambiente del muscolo scheletrico, inteso come matrice extracellulare (ECM). Utilizzando un modello murino di obesità cercheremo di capire se questo può avere un ruolo nella deposizione dell'IMAT e dei processi infiammatori ad esso associati.

Materiali e metodi

Sia biopsie muscolari sia campioni di siero sono stati prelevati da pazienti sani, obesi normoglicemici e obesi diabetici. Mediante l'utilizzo di analisi di Real-time PCR le prime sono state analizzate per i principali marcatori infiammatori, mentre i secondi per i principali miRNA muscolari circolanti.
Nella seconda parte dello studio, invece, è stato settato un protocollo di decellularizzazione del tipo detergente enzimatico su quadricipiti murini di topi wild type (C57BL6J) e di topi ob/ob (B6.Cg-Lep$^{ob/J}$) e i campioni ottenuti sono stati caratterizzati per il contenuto di DNA e le componenti strutturali della matrice. In seguito è stato creato un modello di perdita consistente di massa muscolare in topi wild type (wt) ed è stata impiantata nelle sede di danno una porzione di matrice proveniente da topi wt o ob/ob. La capacità delle diverse matrici di essere rimodellate e riassorbite è stata analizzata dopo 7, 15 e 30 giorni mediante analisi di immunofluorescenza e molecolari.

Risultati e discussione

L'mRNA estratto da 3 biopsie di retto addominale di pazienti obesi normoglicemici e obesi diabetici, insieme a 3 biopsie di muscolo peroniere di soggetti sani indica la presenza di una maggiore espressione dei geni pro-infiammatori sia nei soggetti obesi normoglicemici sia diabetici in confronto a quelli sani. Tuttavia, in contrasto con quanto ci aspettavamo, i pazienti diabetici che erano in trattamento con Metformina da almeno 1 anno mostravano un grado infiammatorio inferiore. Osservando poi i livelli di miRNA 133a, miR133b e miR1 presenti nel siero di una coorte di pazienti

sani, obesi normoglicemici e obesi diabetici abbiano notato lo stesso andamento descritto in precedenza per le biopsie muscolari. Questo ci suggerisce una possibile correlazione diretta tra infiammazione muscolare e rilascio di questi miRNA circolanti, che in futuro potranno essere utilizzati come marcatori della condizione muscolare del paziente.

La decellularizzazione dei quadricipiti wt e ob/ob non ha evidenziato differenze strutturali tra le due matrici. Inoltre il trapianto in vivo di entrambe ha indotto a 7 giorni una forte migrazione cellulare all'interfaccia tra tessuto nativo e matrice, la quale diminuisce a 15 e 30 giorni dopo impianto. Cellule macrofagiche ($CD68^+$) sono state trovate in entrambe le matrici, soprattutto nelle aree attorno ai punti di sutura e all'interfaccia con il tessuto nativo, tuttavia a nessun time point è evidente una condizione infiammatoria nella parte più interna del muscolo nativo. La colorazione Alcian Blue e quella della Tricromica di Masson hanno mostrato un' induzione nella deposizione di glicosamminoglicani e di collagene simile tra le due matrici. Nello specifico, abbiamo osservato, quindi, che una matrice derivante da un donatore affetto da malattia metabolica non è in grado di indurre un'alterazione nella deposizione di componenti strutturali ma promuove una prematura risposta infiammatoria di tipo M2 che si riduce o stabilizza dopo 30 giorni dall'impianto. Al contrario, la matrice proveniente da topi sani induce una ricostruzione del tessuto più ritardata ma che porta a una miglior e completa rigenerazione. Nessuna differenza, infine, è stata osservata in termini di attivazione e modulazione dei segnali miogenici e adipogenici per entrambi gli impianti.

ABSTRACT

Introduction

The optimal condition for skeletal muscle function is represented by an efficient activation of processes that regulate muscle development, growth, regeneration and metabolism. When the balance among these events is missing, a pathological condition arise. In particular, loss or decrease of skeletal muscle function and mass is linked with severe health diseases such as muscle dystrophies, cancer, obesity and aging process.

In this context, sarcopenic obesity, a metabolic disorder followed by atrophy of muscle fibres and reduction of stem cell reservoir (satellite cells in muscle) is associated with increasing ectopic adipose tissue, impairing glucose tolerance and decreasing strength and mobility in old adults.

This excess of fatty acids accumulated in several other organs, including skeletal muscle, induces metabolic dysfunctions, β-oxidative alterations, increase of ROS production, lipotoxicity and insulin resistance. Moreover this intermuscular adipose tissue (IMAT) acts as chemoattractant for inflammatory cells, chiefly macrophages, which produce high amount of pro-inflammatory cytokines (TNF-α, IL-6, IL-1, INFγ) and low of anti-inflammatory cytokines (IL-4, IL-10) resulting in chronic low-grade systemic inflammation and muscle loss.

Aims

The aim of this work is to investigate the origin of intermuscular fat and the complex mechanisms regulating the crosstalk with the surrounding muscle. In the first part of the study we try to understand the differences in muscle inflammation in obese subjects both normoglycemic and diabetic versus healthy patients using muscle biopsies. Moreover, in the same groups of patients, we attempt to identify serum microRNAs as possible useful markers of muscle alterations in presence of obesity. Because it is well known that in chronic diseases, as obesity and diabetes, multifactorial components contribute to the pathology, we decided to investigate the

microenvironment of skeletal muscle, represented by extracellular matrix (ECM). We aim to understand if it could have had a role in the deposition of IMAT and on associated inflammatory processes using an obese mouse model.

Material and methods

From healthy and obese patients either normoglycemic or diabetic, both muscle biopsies and serum samples were collected. By Real-time PCR the first were analysed for selected inflammation markers, whereas the second for the principal muscle circulating miRNAs.

In the second part of the study, a detergent-enzymatic decellularization protocol for wild type (C57BL6J) and ob/ob (B6.Cg-Lep$^{ob/J}$) murine quadriceps were set and samples were characterized for DNA content and ECM structure preservation. After that, a volumetric muscle loss model on wild-type mice was created and ECMs from wt or ob/ob quadriceps mice were implanted. The ability of the matrices to be remodelled and reabsorbed was evaluated by immunofluorescence and molecular analysis after 7, 15 and 30 days.

Results and discussion

mRNA from three human *rectus abdomins* biopsies from obese patients both normoglycemic and diabetic and three peroneal muscle biopsies from healthy subjects indicate an increase in pro-inflammatory gene expression both in normoglycemic and diabetic patients in comparison with the controls. However, in contrast to what we expected, diabetic subjects, that were under Metformin treatment from at least 1 year, showed a reduction of inflammation. The serum miR133a, miR133b and miR1 levels of healthy and obese patients both normoglycemic and diabetic, display the same trend previously described for muscle biopsies. This suggests a possible direct correlation between muscle inflammation and the release of these circulating miRNAs, which could be used in the future as indicative markers of patient muscle alterations.

On the other hand, the decellularization of wild type (wt) and ob/ob quadriceps did not show significant structural differences between the two samples. In vivo transplantation of the two decellularized muscle matrix (ECMs) in wt injured mice induced after 7 days a strong cells migration in the interface between the native tissue and the matrix that gradually diminished after 15 and 30 days. . Pan macrophages cells ($CD68^+$ cells) were found in both ECM implantation, mainly in the area around the stitches and in the interface between the matrix and the native tissue, but in the inner part of the recipient absence of inflammatory infiltrate was evident at all time points. Alcian blue and Masson's Trichrome stains highlighted similar GAG deposition and collagen components between wt and ob/ob donor ECM. In particular we observed that the scaffold derived from donor affected by a metabolic disease did no induce alteration in structural matrix deposition but promoted a premature M2 inflammation that was reduced or stabilised after 30 days. On the contrary healthy ECM in wt mice start later the tissue rebuilding leading to a more complete regeneration. No differences were also observed in activation or modulation of myogenic and adipogenic pathways after both implantations.

ABBREVIATIONS

ICM: inner cell mass
SC: satellite cell
ECM: extracellular matrix
MRF: myogenic regulatory factors
MyHC: myosin heavy chain
MYF5: myogenic transcription factor 5
MYOD: myoblast determination protein
RISC: RNA- induced silencing complex
UTR: untranslated region
APA: polyadenilation
PGs: proteoglycans
GAGs: glycosaminoglycans
FN: fibronectin
VEGF: vascular endothelial growth factor
FGF: fibroblast growth factor
TGFβ: transforming growth factor
VML: volumetric muscle loss
WAT: white adipose tissue
BAT: brown adipose tissue
VAT: visceral adipose tissue
SAT: subcutaneous adipose tissue
UCP1: uncoupling protein 1
ECHO: Commission on Ending Childhood Obesity
T2DM: type 2 diabetes mellitus
CVD: cardiovascular diseases
NIH: national Institute of Health
LGS: sleeve gastresctomy
RYGF: Roux-en-Y gastric bypass
IMAT: intermuscular adipose tissue
FAP: fibro-adipogenic precursor cell
IMTG: intramyocellular triglycerides
DAG: diacilglycerol
CER: ceramides
EWGSOP: European Working Group on Sarcopenia in Older People
AMPK: AMP- activated protein kinase
iNOS: inducible nitric oxide synthase
COX: cyclooxygenase
WT: wild type
OB/OB: obese
PBS: phosphate buffered saline
DET: detergent enzymatic treatment
DAPI: 4',6-diamino-2-phenylindole

H&E: haematoxylin and eosin
MT: Masson's Trichrome
AB: Alcian Blue
SEM: scanning electron microscopy
PFA: paraformaldehyde
TA: tibialis anterior
BMI: body max index

INTRODUCTION

1.1 Skeletal muscle

Skeletal muscle represents approximately 40% of the body weight in lean men and women and, therefore, constitutes the largest organ in non-obese human [1]. It is mainly composed of water (75%), protein (20%) and other important substances like inorganic salt, minerals, fat and carbohydrates (5%). Normal skeletal muscle has elongated muscle fibers with multiple cell nuclei in sub-sarcolemma position and cytoplasm (called sarcoplasm) rich in myofibrils. Every single fiber is surrounded by a cell membrane (sarcolemma), associated with several proteins physically connected to the internal myofilament structure. The set of muscle fibers is organized in fascicles surrounded by thin connective tissue (perimysium) and the global muscle bulk is also bounded by collagen-filled connective tissue (epimysium) (Fig. 1) [2, 3].

Muscle fibers can be classified on: myoglobin content that contributes to the colour of the muscle (white or red), contractile properties, speed of shortening (fast or slow), degree of fatigability, predominance of certain metabolic or enzymatic pathways (oxidative or glycolytic), calcium handling by the sarcoplasmic reticulum and protein isoform expression. The most important types are: type I (slow, oxidative, fatigue-resistant), IIA (fast, oxidative, intermediate metabolic properties) and IIx (fastest, glycolytic, fatigable).

The proper functions of skeletal muscle are: a) to convert chemical into mechanical energy in order to generate force and power and sustain other organs; b) to contribute to basal energy metabolism, serving as storage for substrates such as amino acids and carbohydrates, maintaining core temperature or consuming the majority of oxygen during exercise [3].

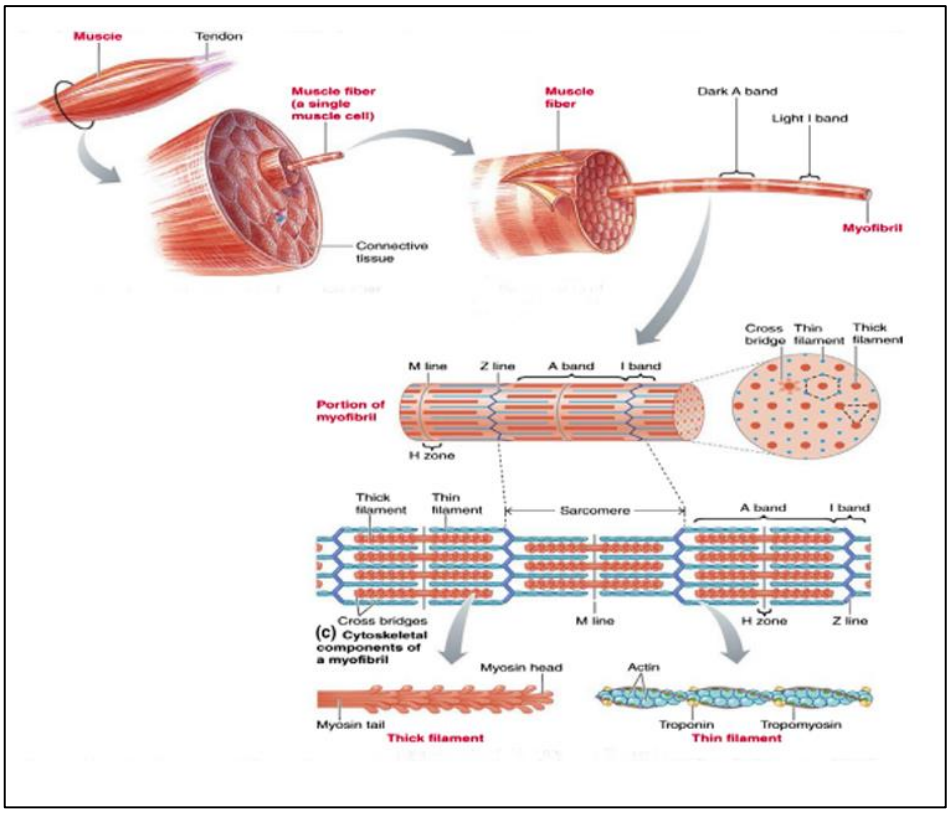

Fig. 1:Skeletal muscle structure (from Frontera et al, 2015) [3].

1.2 Stem cells

Stem cells are considered cells with the unlimited capacity to generate daughter cells genetically identical to the mother (self-renewal) or with the ability to enter into a committed pathway and differentiate into various cell types [4].

Based on their differentiation capacity they could be classified as:

- totipotent stem cells: able to generate a whole organism by differentiating in all tissue cells and extra-embryonic organs;
- pluripotent stem cells: derived from totipotent stem cells and able to differentiate only in the three germ-layer of the embryo (mesoderm, endoderm, ectoderm). These cells are localized into the inner cell mass (ICM) of the blastocyst;
- multipotent stem cells: cells that can differentiate in some restricted cell types, generally those that constitute the germ layer from which they originate;
- unipotent stem cells: are characterized by the ability to differentiate in only one specific cell type [5].

Depending on the tissue of origin, stem cells may be divided into embryonic, foetal or adult stem cells. The first ones are isolated from the ICM, are identified by the presence of specific markers, such as O*ct4, Sox2, cMyc, Klf4 and Nanog* and, in spite of their ability to be maintained in culture for a long period of time, they are able to induce teratogenicity and rejection after transplantation [6]. The second ones, the foetal stem cells, derive from the foetus itself or from the extra-foetus support structures like placenta, amniotic fluid or amniotic membrane. Because of their great quantity and easy access, their characteristics of pluripotency and their potentiality to differentiate into several committed cells, these cells could be a promising source for new therapeutic approaches [7]. The last ones, adult stem cells, are capable to originate committed cells derived from the tissue in which they are present. These, are primary involved into the growth of the organ and then, at a later stage, into the maintenance of tissue homeostasis [8].

1.2.1 Satellite stem cells

Satellite cells (SC) are adult stem cells with large nuclear-cytoplasmic ratio, small nucleus, few organelles and are located beneath the basal lamina and outside the myofiber plasma membrane [9]. Their number was estimated between 30-35% of muscle cells in the post-natal life to 1-4% in the adult life in mice and humans [10]. SC are, by definition, stem cells in a quiescent state that have the ability to contribute to the muscle homeostasis or be involved in the regeneration and repair process after injury [11].

These cells, like all adult stem cells, are maintained in a quiescent state by specific anatomic structures, named niches, which provide an ideal microenvironment for cell characteristics and survival. These environment cues include growth factors, cytokines, adhesion molecules and extracellular matrix (ECM) released by the various cell types present in muscle tissue. Quiescent SC express high levels of integrin α7, M-cadherin and the glycoprotein CD34 that under homeostatic condition are involved in the adhesion of the cells to the basal lamina and in the sequestration of soluble factors in the immediate cellular microenvironment. In contrast, during muscle regeneration the composition of the niche changes and immune cells,

fibrogenic cells and endothelial cells become involved in the remodelling of the tissue [12].

The niches could operate in two different ways: they can induce an asymmetric or symmetric cell division. In the first case one daughter cell goes away, loses the contact with the niche and feels the effects of differentiation stimuli, whereas the other one remains in the stem cell pool of the niche itself. In the second case, instead, both daughter cells stay in the niche or undertake the committed process [13].

The passage from SC to myofiber consists of specific steps that start from quiescence state and finish with cell fusion. Upon activation, the $PAX7^{+}$ SC enters the myogenic pathway and expresses the early myogenic regulatory factors (MRFs), such as MYF5; when it is time to form myoblasts, markers like MYOD are activated. At this stage, the myoblasts fuse in myotube and Myogenin and Myosin heavy chain (MyHC) proteins are expressed (Fig. 2) [14].

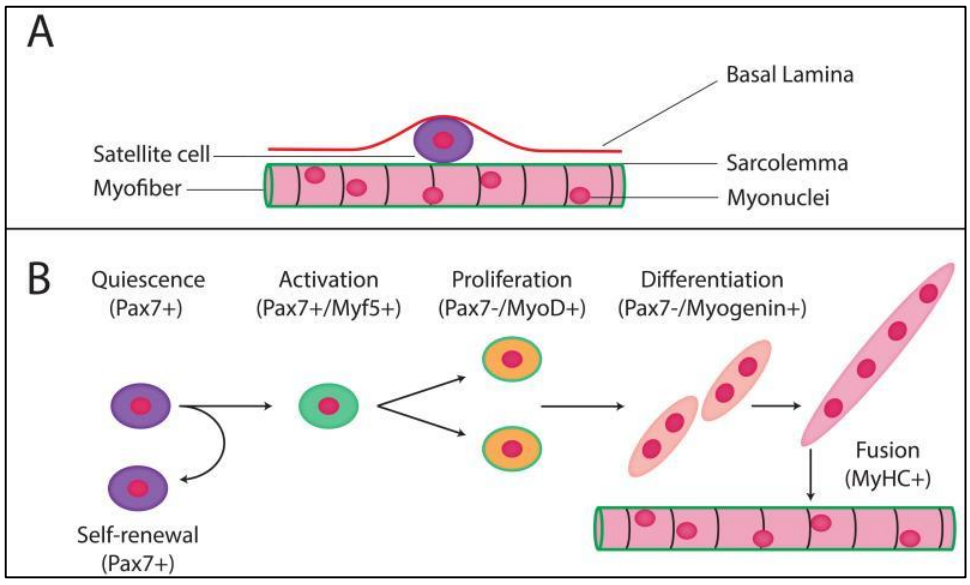

Fig. 2: Satellite cells activation (From Dayanidhi et al.)[14].

1.2.2 Myogenic precursor cells

Maintaining the balance amongst quiescence, activation, proliferation, differentiation and self-renewal is a critical process and involves many signalling mechanisms [14]. SC are considered a homogeneous population of committed muscle progenitors with differences in their gene expression signatures, myogenic differentiation propensity and stemness.

In intact muscle, SC interact with the basal lamina and the sarcolemma, are in a quiescence state and are characterized by the expression of Pax3 and Pax7 markers. After injury these contacts are interrupted and cells are induced, by different stimuli, to be activated and differentiated into a descendent population of muscle committed cells, known as myogenic precursor cells (MPCs). The activation of SC into myoblast involves the up-regulation of the basic helix-loop-helix (bHLH), transcription factor 5 (MYF5), myoblast determination protein (MYOD), myogenin and muscle-specific regulatory factor 4 (MRF4). Together, these myogenic regulatory factors (MRFs) are able to control the myogenic capacity of muscle progenitors to restore damage. The balance between MYOD or MYF5 expression drives the passage through quiescence and differentiation state: predominance of MYOD expression induce SC activation while MYF5 controls their proliferation and delays differentiation. Kuang et al. demonstrated also the presence of heterogenic population within $PAX7^+$ sc based on the expression of MYF5 marker; in particular $PAX7^+/MYF5^-$ cells contributes to the reservoir of the niche, while $PAX7^+/MYF5^+$ cells are committed to differentiation [9, 15, 16].
Upon downregulation of Myf5 and MyoD, the new $myogenin^+$ myoblast cells first fuse to one another generating myotubes with few nuclei and second additional myoblasts incorporate into the nascent myotubes forming a mature myofiber with increased size and expression of contractile proteins [9]. Fusion is then accompanied by the expression of the late muscle differentiation transcription factor MRF4, cytoskeletal proteins such as dystrophin and dystroglycan, as well as functional contractile proteins such as sarcomeric myosin (MyHC). Once fusion is completed, under physiological conditions, the regenerated muscle is morphologically and functionally indistinguishable from undamaged muscle [17].

1.3 microRNA

In eukaryotes multiple types of small RNAs have been evolved to control genetic information. In particular, a class of evolutionally conserved, single-stranded, small (19-23 nucleotides) and non-protein coding class of RNA,

called microRNA, act as post-transcriptional regulators of gene expression in a broad spectrum of animals, plants and viruses [18, 19].

The first miRNA was discovered on *C. Elegans* in 1981 during a genetic screening of the post-embryonic development [20]. The miRNA biogenesis is a multiple step process that takes place in two different cell compartments. miRNA are first transcribed in the cell nucleus from intergenic or intragenic regions by RNA polymerase II to form primary miRNA (1-3kb). These primary miRNAs consists of a stem of 33-35bp, a terminal loop and single-stranded RNA segments at both the 5' and 3' sides and are cleaved in the nucleus by the RNase III enzyme Drosha which crops the stem-loop and releases a small hairpin-shaped RNA of ~65 nucleotides called pre-miRNA. Then the pre-miRNAs are transported to the cytoplasm by Exportin5, where the miRNA maturation can be completed. Here the pre-miRNAs are cleaved into the 18-24 double-stranded oligonucleotides by the RNase III enzyme Dicer into mature double stranded miRNA-miRNA*: one of the strands becomes a mature miRNA and is incorporated into RNA-induced silencing complex (RISC), while the other one is often degraded or plays a functional role in the regulation of miRNA homeostasis. At the end, the RISC complex match perfectly or imperfectly with its complementary mRNA target inducing its degradation or inhibition (Fig.3) [18, 19].

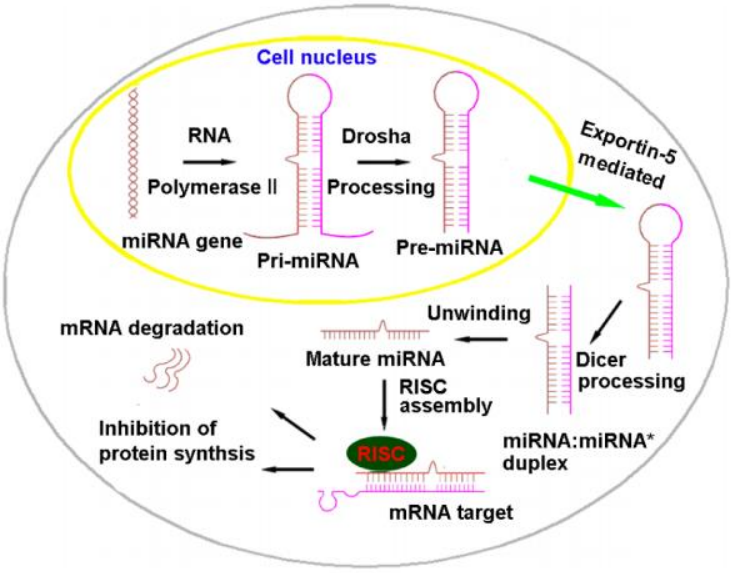

Fig. 3: miRNA biogenesis (from Dong at al.)[19].

miRNA binding sites are usually located in the 3' untranslated region (UTR) of mRNAs and the imperfect pairing of miRNA-mRNA is considered to mediate post-transcriptional silencing more efficiently than pairing within the 5' UTR or coding sequence. Furthermore, 3'UTR heterogeneity caused by SNPs or alternative polyadenilation (APA) impacts miRNA-post transcriptional regulation and permits to have a single gene regulated by multiple miRNA and a single miRNA which might have more than one mRNA target [21].

Increasing evidence indicates that miRNAs play crucial regulatory roles in a vast range of biological processes including early development, cellular differentiation, proliferation and apoptosis [19].

On skeletal muscle, the most important miRNAs, miR1 and miR133a/b with miR206, are called the original myomiRs. These miRNAs are considered muscle specific for their prevalence in skeletal and cardiac muscle and for their central role in the regulation of myogenesis, muscle development and muscle remodelling under the control of myogenic regulatory factors (MRFs) including Myogenin, MyoD and Myf5 [22, 23].

miR-133a has a regulatory role from the earliest differentiation of myogenic stem cells into myoblast and has homeostatic functions for muscle maintenance and protection in mature muscle even after damage and stress. It is expressed both in skeletal and cardiac muscle where mediates mesenchymal lineage commitment by inhibiting differentiation into osteoblasts and chondrocytes in order to control skeletal muscle development [24]. It was also demonstrated its role in the repression of white adipocytes browning and beige adipocytes formation *in vivo* mouse model [25].

miR133b, differs from miR133a in only one nucleotide at the 3'end, is absent in cardiac muscle and has central roles both in homeostatic maintenance of skeletal muscle and in neuromuscular synapse development. For these reasons during myogenesis both miR133a and -133b are upregulated.

Literature evidence suggests that miR133 family could play an opposite role in skeletal muscle myogenesis by repressing Serum Response Factor (SRF) and resulting in promoted proliferation or by suppressing myoblast

proliferation and promoting cells differentiation regulating MAPK. miR133 is also involved in the promotion of sarcomeric actin organization, vascular remodelling, and induction of cell death.

miR1 promotes myogenic differentiation and decreases cell proliferation by silencing HDAC4 gene. In particular, on SC, inhibits *PAX3* and *PAX7* genes inducing myoblast differentiation [24].

Recently, the attention has been directed on the role of these myomiR on human diseases. Since they were easily found circulating in body fluids such as serum, plasma, saliva and other derived from various tissues/organs, they early began considered as novel non-invasive biomarkers for diagnosis of cancer or other disease [26]. For example myomiR sera levels were correlated with the progression of muscle wasting and weakness in type 1 muscular dystrophy (DM1) patients might reflecting the effects of cytokines and growth factors on the degeneration of the muscle [27, 28].

1.4 Extracellular matrix

The ECM is a well-organized network present in all tissues and organs and composed of a mixture of cells and non-cellular components [29]. In mammals, the ECM is composed of around 300 proteins, many of which are fibrous-forming proteins like collagens, elastin, fibronectin, laminins, glycoproteins, proteoglycans (PGs) and glycosaminoglycans (GAGs). The precise composition and specific structure of the ECM vary from tissue to tissue and it is the result of a dynamic, reciprocal, biochemical and biophysical dialogue between various cellular components [30]. However, the main functions are always the same: to provide physical support for tissue integrity and elasticity and to regulate cell behaviour by influencing cell proliferation, survival, differentiation and migration [31, 32]. In particular, the ECM acts as a substrate to facilitate cell adhesion for the formation of tissues and organs, it is a physical barrier between different tissues and it influences many cellular functions through three models: (a) mechanical stimulation from substrates with different stiffness, (b) regulation of soluble factors availability and activity, and (c) intracellular signalling activated by cell adhesion molecules [33].

The different components of ECM are organized in a 3D structure which can be divided into two types: one presents in the interstitial and one in the basal lamina (Fig. 4). The first one surrounds cells and is mainly composed of collagen I and fibronectin; the second one, instead, consists of collagen IV, laminins, heparan sulphate proteoglycans and other proteins synthesized by epithelial and endothelial cells and controls cell organization and differentiation through interactions with cell surface receptors [31].

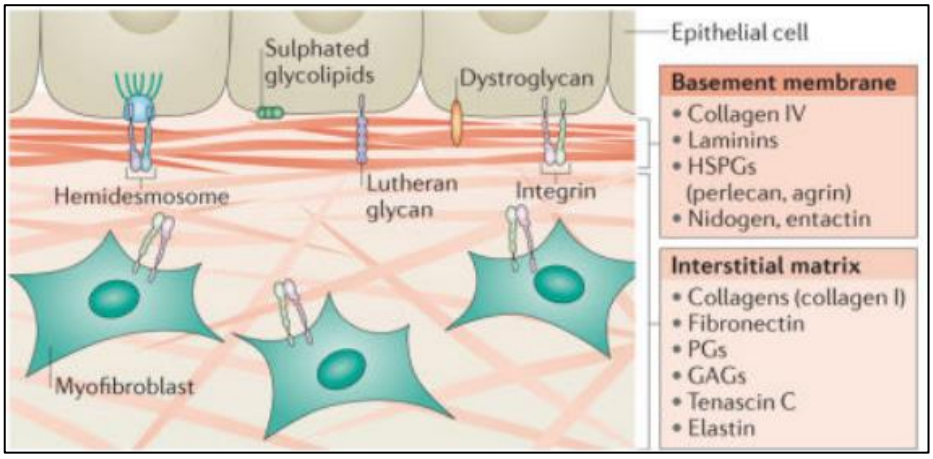

Fig. 4: Mammalian ECM types (from Bonnans at al.) [31].

Proteoglycans are the most important structural and functional molecules in tissue. They are core proteins with attached one or more GAG chains of the same or different type. PGs fill the extracellular interstitial spaces and confer hydration functions by sequestering water within the tissue. They also interact with numerous growth factors, cytokines and chemokines, cell surface receptors both via their core or GAG chains. Due to these abilities PGs are also important for ECM organization contributing to the formation of the scaffold and the cell embedding within [29, 31].

Collagen is the most abundant protein in the body representing up to 30% of the total proteins in humans and it is synthetized and secreted by fibroblasts, endothelial cells and epithelial cells. Collagen superfamily is composed of 28 sub-types, all different from each other both in structure and properties. They are classified into fibrillar and non-fibrillar forms and both of them provides tensile strengths to the ECM limiting the distensibility of tissues. Collagens provide tensile strength, regulate cell adhesion and support cell chemotaxis and migration. The dominant form, Collagen type I, is presents

particularly in tendons and skin, whereas type II is the principal form within the walls of blood vessels. Mutations in collagen and the remodelling of the ECM that occur during several pathologies could contribute to malignant progression of different diseases [29, 30, 32].

Elastin is another structural protein with a linked role to collagen. In fact, elastin acts with its hydrophobic domain in that tissues which needed repeating stretching forces such as skin, blood vessels, lungs or that needed elastic properties.

Fibronectin (FN) is the second component of ECM for abundance and is ubiquitously expressed in the tissues with functions in the development of vertebrates. It is located in the basal lamina and has a key role in cells adhesion and in the response after injury. The protein is synthetized in two different forms: as soluble FN present in plasma and circulating in the blood or as a cellular protein that is generated by fibroblasts [32].

Components of the ECM contain various interacting sites which make them able to bind numerous cell receptors, such as integrins, and to elicit signal transduction and regulate gene transcription in multiple biological activities essential for the development and homeostasis of the tissues. The ECM can also sequester and release several cytokines, chemokines and growth factors, like vascular endothelial growth factor (VEGF), fibroblast growth factor (FGF) and transforming growth factor β (TGF β) which also regulate the ECM architecture and cell behaviour [31].

Loss of functions and modification in ECM molecules are often associated with pathological conditions. For example, greater stiffness observed in aged tissues has been attributed to unnecessary collagen cross-linking and results in compromised ECM biochemical properties: the tissue is mechanically weaker and less elastic but also more rigid. Moreover, in the condition of obesity, deregulations in ECM remodelling are confirmed in both adipose tissue and skeletal muscle [34]. The positive effect of weight loss on skeletal muscle has been proved mainly in clinical studies [35], but the characteristics of muscle SC and ECM in obese and slimmed down patients are still to be investigated.

1.5 Volumetric muscle loss (VML)

Skeletal muscle has an innate capacity to auto-regenerate and repair after mild injures like strains, contusions and lacerations. This mechanism is directed by the native architecture of the basal lamina and involves SC, which are able to leave their quiescent state and enter into myogenic commitment. When damage exceeds 20% of the total muscle volume (for example after a trauma, an infection or a surgical resection) and the regenerative capabilities are compromised, the endogenous mechanisms are insufficient. At the beginning, this volumetric muscle loss (VML) was observed in soldiers returning from war in which explosions made them disabled. VML could be divided in two categories: one characterized by a partial compartment loss and one in which there is also the loss of blood vessels and nerve connections [36]. For both conditions, the current standard of care is the transfer of autologous muscle flap but it is an extremely invasive procedure that could cause several morbidity and graft failure secondary to tissue necrosis [37-40].

Many engineering approaches were tested but the most promising is represented by the transplantation of an acellular scaffold with or without a stem/progenitor cell. The idea that the degradation of the implanted biological scaffold could release growth factors, peptides, fragments that can interact with the host and promote a pro-regenerative microenvironment is at the base of this new regenerative medicine [41]. The ECM could be derived from different sources and species but the aim is always to obtain a 3D structure lacking of immunogenicity but preserving the structural and biological functions. Also the differentiation status of the cells used is very important for the recovery of the muscle functionality. Up to now, many stem cell types have been evaluated, including embryonic stem cells [42], pluripotent stem cells [43], satellite and myoblast cells [44, 45], but the problems remain the difficulty to *in vitro* expand the muscle precursors while maintaining their myogenic phenotype and to obtain *in vivo* new functional muscle fibers.

For example, in 2003 Corona and colleagues demonstrated that transplantation of a muscle ECM in a mouse model of VML can improve the rate of muscle strength and that an extensive deposition of collagen, obtained

after ECM implantation, can protect the remaining muscle from the injury stress and fibrosis. However the authors were not able to explain why they did not found new muscle fibre regeneration even after bone marrow-derived mesenchyme stem cells injection [41]. So many questions about ECM physio-pathological role, its contribution in muscle regeneration and possible employment in tissue reconstruction are still open.

1.6 Decellularization

The constantly growing need for donor tissue and organs has induced scientists to find new approaches of tissue engineering and regenerative biomaterials for transplantation. Tissue engineering is defined as the combination of biological, chemical and physical principles for the development of biological scaffolds which are able to repair, maintain or improve tissues and whole organs using cells, biomaterials and factors alone or in combination [46]. The most promising strategy is the use of a biological scaffold derived via decellularization of mammalian tissue. With this technique, cells and debris were eliminated while biochemical composition, biological activity, three-dimensional organization and integrity of the ECM were preserved. Furthermore, it allows to obtain scaffold for allogenic and xenogenic transplantation minimizing the possible immune rejection, avoiding the immunosuppressive drugs administration, and reducing disease transmission. Moreover, a lot of evidence suggests that a variety of important biological important activity can be attributed to the degradation of the native ECM scaffold structure and its associated release of soluble bioactive peptides.[47] Despite these advantages, the structure of the transplantable matrix must be non-toxic, non-pathogenic, biodegradable, able to allow cell adhesion and optimal for cell growth, proliferation and migration in order to facilitate new tissue formation [48].

The tissue or organ, the species of origin, the decellularized method and the terminal sterilization of the scaffold vary widely based on cell density, matrix density and geometric considerations including tissue thickness and shape. The aim of decellularization is, on one hand, to remove all cell components and antigens eliminating the risk of immunological rejection, and on the

other hand, to preserve the three dimensional ultrastructure and composition of the native ECM [49].

Several methods of decellularization are being evaluated and the most common start with lysing the cell membrane by physical treatment or ionic solution, then dissociating the cellular components by using enzymatic treatment and detergent for the solubilisation of cytoplasm and nuclear elements, and finally removing cellular debris [50].

Physical methods use freezing and thawing cycles which minimize the amounts of chemical agents required for decellularization, agitation by magnetic stir plate, orbital shaker or a low profile roller, pressure which improve the efficiency of delivering cell-lysing agents into tissue and forcing cellular debris out, sonication and electroporation. All of these practices tear the cell membrane and induce the release of the cellular contents. Enzymatic methods, instead, comprise trypsin, collagenase, alpha-galactosidase, nucleases, phospholipases A2, lipase and dispase and are advantageous because of their specificity for biological substrate. Chemical treatments, finally, include acid, alcohols, ionic and non-ionic detergents and hypertonic or hypotonic solution that disrupt cell membranes and the bonds responsible for intracellular and extracellular connection [48, 49, 51].

There are two technical procedures of decellularization: the whole organ perfusion and the immersion with agitation. The first consists into anterograde and retrograde perfusion using vasculature tree because it largely preserves the 3D architecture of the organs. This is a particularly efficient method for complex organs like heart [52], lung [53], liver [54] and kidney [55], but it is not possible to use it for small tissues or tissues lacking of easily accessible vasculature. For these samples, instead, the most common approach is immersion and agitation in decellularization agents. Several tissues were efficiently decellularized with this protocol, such as skeletal muscle [56], heart valves [57], blood vessels [58], trachea [59] and urinary bladder [60].

One of the most important parameters of implant biocompatibility is cytocompatibility that measures the qualitative and quantitative aspects of the impact of the scaffold on the host. This aspect is important because the

decellularization agents can also cause damage to the ECM structure and remove growth factors of the ECM itself but also an insufficient decellularization can induce a strong inflammatory response [49]. For these reasons the ECM scaffolds must follow some criteria: (1) to have an amount <50ng of dsDNA per mg ECM dry weight, (2) to have the remaining dsDNA <200bp fragment length and (3) to have no visible nuclear material in tissue sections stained with DAPI or H&E [61].

Up to now, complete removal of all cells is not possible and the decellularization protocol inevitably causes some disruption of matrix architecture, orientation and surface ligand. However in literature there are numerous naturally ECM devices which have received the approval by FDA for human clinical application like *GraftJacket* that is a commercial product prepared by the decellularization of human dermis, *CuffPatch* derived by the decellularization of porcine sub-intestinal submucosa or *CardioCel* that is an acellular pericardium-based product stabilized with gluteraldehyde [62].

1.7 Adipose tissue, obesity and metabolic syndrome

In human body, adipose tissue is one of the most important endocrine organ that plays a central role in several biological process such as energy homeostasis, feeding behaviour, energy expenditure, insulin sensitivity and inflammation [63]. It is composed not only by adipocytes but also by stromal-vascular cells, leukocytes, macrophages and pre-adipocytes, which contribute to the structural integrity of the tissue.

In mammals, there are two main classes of adipose tissues, each of them with different functions: white adipose tissue (WAT) is the primary site of energy storage and of release of hormones and cytokines that modulate whole-body metabolism and insulin resistance; whereas brown adipose tissue (BAT) has central role in the thermogenesis via mitochondrial uncoupling of oxidative phosphorylation of free fatty acids [64, 65]. In particular, in human, WAT is located in many distinct depots, one of which is intra-abdominal (VAT) and one is subcutaneous (SAT). Both of them are characterized by the presence of a single large lipid droplet within the cells which pushes the nucleus against the plasma membrane. BAT, instead, has multilocular cells and containing

many smaller lipid droplets with a centrally located nucleus and with an elevated number of mitochondria [65, 66].

Despite the historical concept that white and brown adipocytes arise from the same mesenchymal precursor cells, lineage-tracing experiments on mice demonstrate that the two cell lines have different origins: BAT is more closely related to skeletal muscle cells, having in common the progenitor cells expressing the early muscle marker myogenic factor (myf5), whereas WAT origins from myf negative precursors cells. (Fig. 5)[67]. This was shown for the first time in mouse knockout model for PRDM16, the must regulator of the brown fat program, in which an absent expression of this transcriptional cofactor induces a switch of the myoblast to brown fat [68].

Furthermore, in the last few years it was demonstrated the presence, within adipose tissue, of a new cell population similar to brown adipocytes but with different origin. These cells, called beige adipocytes, derived from Myf negative cells by transdifferentiation of white adipocytes and show expression of the uncoupling protein 1 (UCP1) after a prolonged cold exposure or in response to β-adrenergic signalling [69].

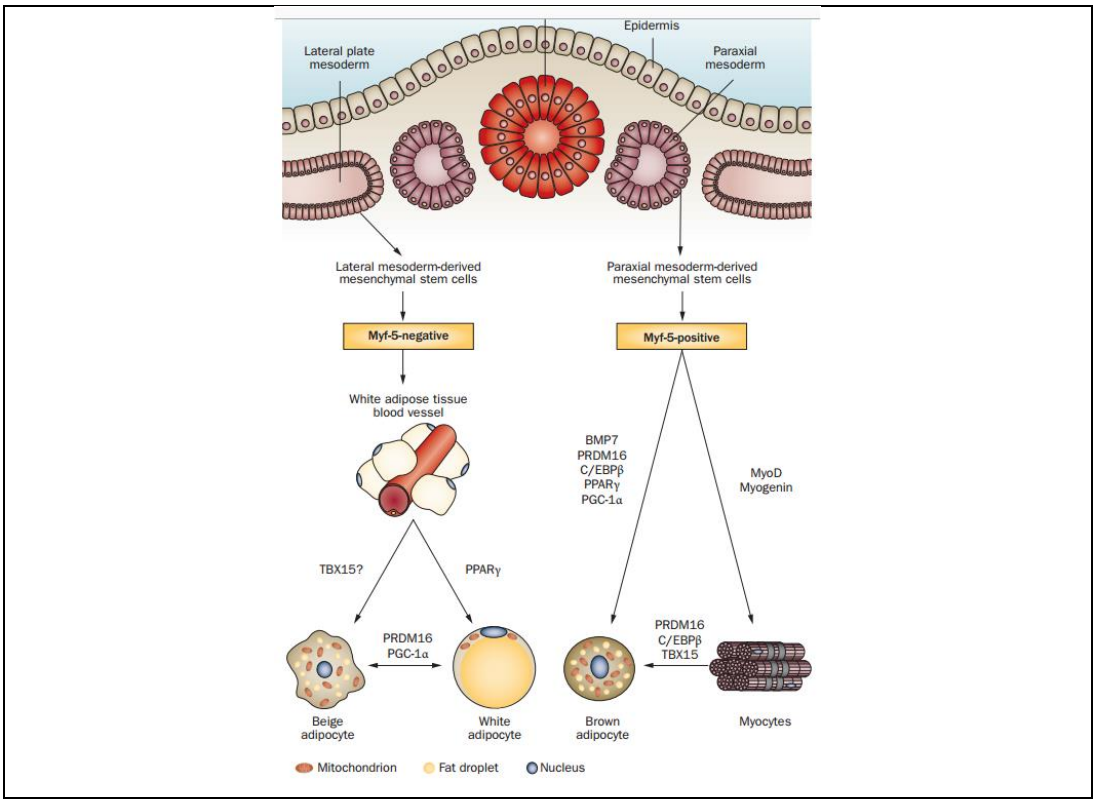

Fig. 5: Origin and development of white and brown adipocytes [65].

Obesity is, by definition, a state of increased body weight, in particular adipose tissue, sufficient to produce adverse health consequences. The storage of energy as triglyceride in adipose tissue influence body weight and composition and is determined by genetic, environmental and psychosocial factors. Thus, these elements can change the positive balance between energy intake and expenditure inducing fat accumulation [70]. Although the role of genes in body fat regulation, the two most important causal factors are considered urbanization and globalization of food production and marketing. The global nature of modern commerce and the marketing campaigns permitted, in fact, the introduction of low-cost and energy-dense foods also in developing countries [71].

Nowadays, obesity is considered one of the biggest problems involving health and public spending because of its role in many metabolic disorders and comorbidities such as type 2 diabetes, cardiovascular diseases, hypertension, insulin resistance and cancer. The Commission on Ending Childhood Obesity (ECHO) presents on January 2016 its last report in which draws attention to the alarming rise of childhood obesity since at least 41 million children younger than 5 years are overweight or obese [72].

However, recently it was demonstrated that not all obese patients have the same risk to developing more complications and comorbidities; in particular individuals with peripheral obesity, for example with distributed subcutaneously in the gluteo-femoral region, have little or no risk of the common medical complications of obesity, whereas individuals with central obesity, like fat accumulated in visceral depots, are prone to these complications [73]. This abdominal obesity in conjunction with atherogenic dyslipidemia, raised blood pressure, insulin resistance, proinfiammatory state and prothrombotic state are the six components individuated by the National Cholesterol Education Program's Adult Treatment Panel III (ATP III) as indicative of the metabolic syndrome and they are able to increase five times the risks of type 2 diabetes mellitus (T2DM) and three times the risk of developing cardiovascular diseases (CVD) in human patients [74, 75]. Therefore the importance to understand the mechanisms involved during obesity has become everyday more relevant.

1.8 Bariatric surgery

Bariatric surgery is the most effective treatment for certain high risk patients that are indicated by the National Institutes of Health (NIH) as having a clinically sever obesity. The use of this approach is indicated for those patients who do not achieve a significant weight reduction with therapeutic diet or pharmacotherapy. It is also demonstrated that surgery has beneficial effects thanks to its linking to hyperglycemia remission in patients with type 2 diabetes [76, 77]. The operations can be divided into two categories: malabsorptive or restrictive or a combination of both. The most commonly performed are sleeve gastrectomy (LSG) and Roux-en-Y gastric bypass (RYGB); the first ones is based on a restriction of food intake, whereas the second ones on a decrease of calories absorption. Furthermore, both of them had similar efficacy in the weight reduction [78].

In particular, the sleeve gastrectomy, surgery whose all patients used in this work underwent after medical education, involves a vertical transection of the stomach, creating a tubular channel. At present, LSG is the first choice of surgeons because it does not necessitate to the creation of any new anastomoses, decreasing the risk of ischemic complications and the laparoscopic procedure reduces the potential post-operative infections (Fig. 6) [79].

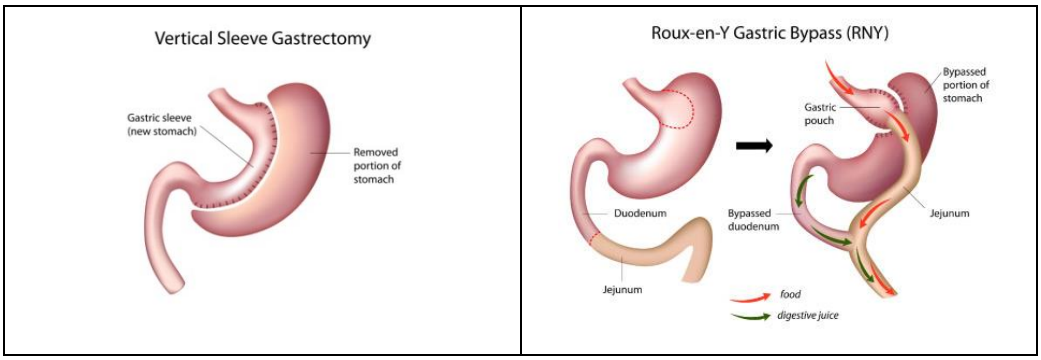

Fig. 6: Most common bariatric surgery (University of Illinois website).

1.9 Intermuscular adipose tissue (IMAT)

The presence of adipose tissue outside of visceral and subcutaneous locations is often associated with chronic inflammation, impaired glucose tolerance, increased total cholesterol and decrease in strength and mobility in older

adults (Fig. 7) [80]. Because its elevate energy expenditures, skeletal muscle is one of the most important organ involves in the ectopic fat deposition.

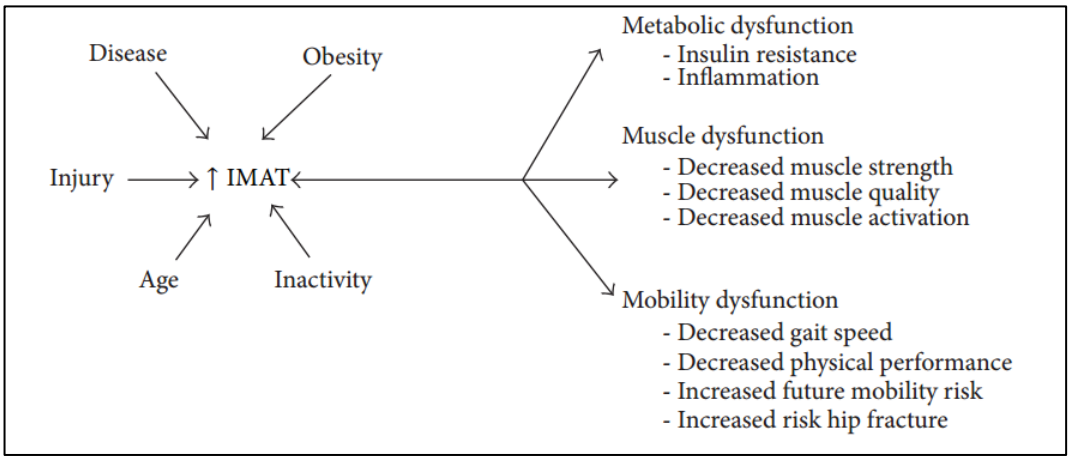

Fig. 7: Increased level of IMAT is correlated with several metabolic, muscle and mobility dysfunction [80].

Muscle fat depots are found in several diseases like myopathies, neurogenic atrophy, type II diabetes, obesity and aging; they include adipocytes between muscle groups (intermuscular adipose tissue) and between muscle fascia (intramuscular adipose tissue), and are characterized by intramiocellular triglycerides, cholesterol ester and the expression of PPARγ, leptin and adiponectin proteins [81].

Many cell types derived from different mesenchymal progenitors can contribute to ectopic adipose tissue formation. These are satellite stem cells, fibro-adipogenic precursors cells (FAP), myoendothelial cells, pericytes, mesangioblasts and fibroblasts. Furthermore, the two cell classes mostly involved seem to be the non-myogenic SCs, which have the capacity to differentiate into adipocytes, express adipocytes-specific genes and accumulate lipids [81] and FAPs, which are able to facilitate myogenesis in co-culture [82], but also possess an intrinsic adipogenic and fibrogenic potential and are capable to impair insulin action in a paracrine manner [83, 84].

It is also important underline how the differentiation of multipotent stem cells into different lineage can be influenced by their interactions with the ECM. In healthy mice, it was demonstrated the presence of abundant

adipocytes after mesh material implanted between muscle fibers indicating that a damage of the ECM can contribute to the adipogenesis process [85].
In the last few years, it was also demonstrated that the intramyocellular triglycerides (IMTG) are not the cause of the insulin resistance [86], but most probably the subcellular localization and composition of diacylglycerol (DAG) and ceramides (CER) as well as their stereospecificity might play an important role in the impediment of insulin action [84].
However, the exact role of ECM on the IMAT development and the onset of related-comorbidities or the influence of environment in muscle cells differentiation into adipocytes remain to be investigated.

1.10 Aging, Sarcopenia and Sarcopenic obesity

Aging is a physiological body evolution that is characterized by a decline in function and number of resident tissue cells and by a delayed response to tissue perturbations or damages [87]. Aging affect especially adult stem cells, which by definition, are able to self-renew and to differentiate into multiple cell lines within the tissue. These cells, despite their phenotypes, have many common characteristics like: telomerase expression during self-renewal, passage from quiescent to activate state, structured chromatin, unique metabolic requirements and a residence within a niche that regulate their behaviour [88]. Strong evidences indicate that a telomere or DNA damages induced by exogenous (UV, radiation, chemical agents) or endogenous sources (ROS), epigenetic alterations as DNA methylation and histone modifications, perturbations of the protein degradation by the proteasome or autophagic systems, and modifications of the structural support or the paracrine signalling released by the niche, can contribute to cells aging and organism-associated diseases [89].
When aging is associated to loss of skeletal muscle mass, and in particular with a decline of type II muscle fibres, the resulted condition is called sarcopenia. This term was postulated for the first time in 1997 by Rosenberg [90], but several new definitions have been suggested in the following years. For example, in 2010 the European Working Group on Sarcopenia in Older People (EWGSOP) developed a practical definition indicating sarcopenia as "*a*

syndrome characterized by progressive and generalized loss of skeletal muscle mass and strength with a risk of adverse outcomes such as physical disability, poor quality of life and death" [91]. This situation is theorized to be a multifactorial process promoted by inflammation, insulin resistance, oxidative stress, disuse, chronic disease, altered endocrine function or malnutrition and it is also associated with metabolic impairment and cardiovascular risk. Furthermore, aging, together with sarcopenic syndrome, is associated with increase visceral adiposity and redistribution of body fat into ectopic depots. This disorder is describe as sarcopenic obesity and its ethiopathogenesis is correlated by many factors such as lifestyle (diet, physical activity), hormones (insulin, growth factors), immunological factors (pro-inflammatory cytokines) and oxidative stress (Fig.8) [92].

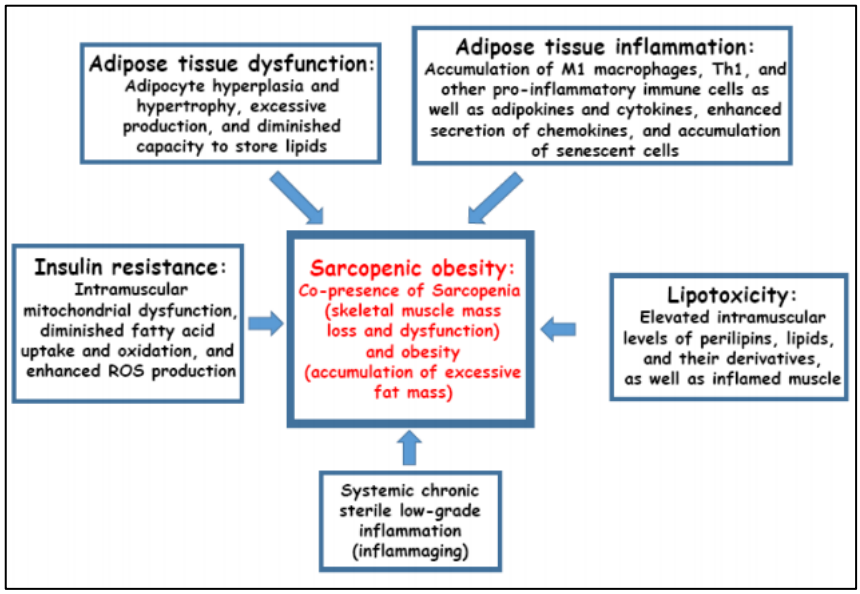

Fig.8: Schematic representation of the mechanisms presumably involved in sarcopenic obesity pathogenesis [93].

Studies in mice and humans demonstrate that obesity is associated with low-chronic inflammation; adipose tissue, in fact, secrete pro-inflammatory (TNFα, IL-1β, IL-6) and anti-inflammatory cytokines (adiponectin and IL-10) which alter insulin sensitivity and it is characterized by macrophage infiltration which control the release of these cytokines and consequently the lipolysis or gluconeogenesis [94]. Thus, one of the theories hypothesized to explain the mechanisms involved in sarcopenic obesity said that it depends by senescent fat macrophages and high fat- diet which increased oxidative

stress and inflammation and resulting in muscle mitochondrial damage [95]. However, further studies are needed to better explain how and why the sarcopenic obesity arises, especially in older adults.

At now, the only treatment for this pathology is focus on two different aspects: weight management, which has the aim to reduce intra-abdominal fat through diet restriction, and physical activity and nutritional supplementation to preserve muscle mass and strength [92].

1.11 Skeletal muscle inflammation

As we said above, loss of muscle, sarcopenia and sarcopenic obesity are all conditions associated to chronic inflammation. In most tissues, like skeletal muscle, there is, in fact, a population of resident immune cells, which increase in pathophysiological situations. In physiological condition, the roles of monocytes/macrophages resident in the tissue are multiple: phagocytosis cells debris or foreign particles and antigen presentation; secretion of enzymes and molecules useful to fight pathogens and production of cytokines and growth factors that act as chemoattractive for additional immune cells [96]. Whereas, in pathological conditions like the presence of intramuscular lipids, it is observed an elevated concentrations of pro-inflammatory cytokines (TNF-α, IL-6, IL-1, INFγ) and a reduction of anti-inflammatory cytokines (IL-4, IL-10) released by resident macrophages, which resulting in chronic low-grade systemic inflammation [97].

Systemic inflammation was demonstrated to reduce rates of protein synthesis and enhance protein breakdown not only activating catabolic pathways but also by downregulating the anabolic ones. All of these events result in the loss of muscle mass [98].

The interaction and modulation between immune cells and satellite cells present in muscle are different during acute events (like a trauma) or chronic conditions (such as sarcopenia). In the presence of trauma, the inflammatory process is finely controlled and the injury is followed by local increase of neutrophils activation. These cells contribute to muscle regeneration and myofiber remodelling phagocyting cellular and matrix debris and dead cells, recruiting and supporting the proliferation of tissue progenitor cells,

inducing vascularization and releasing pro-inflammatory cytokines that reach their maximal concentration after 24h [99]. During this brief period, TNFα, INFγ and IL-1β promote also monocytes differentiation to M1 macrophage phenotype, whose concentration increases and initiates the muscle repair. Subsequently, about 122-144h post-injury, there is an increase in number of anti-inflammatory and pro-myogenic M2 macrophages that contribute to the later stages of regeneration through satellite cells activation [100].

During systemic inflammation, instead, there is a constant low-grade activation of cytokine-producing cells or a dysregulation of cytokine response, which convert satellite cells into fibrogenic lineage and driving uncontrolled wound healing and fibrosis [98]. In presence of conditions like obesity and type 2 diabetes it is also demonstrated an increase of TNFα and IL-6 concentrations that interfere with insulin action by suppressing insulin signalling transduction and causing insulin resistance [101].

1.12 Metformin

Metformin is a pleiotropic drug mainly used for the treatment of type 2 diabetes thanks to its hypoglyceminc effect. It acts improving the sensitivity of organs to insulin, chiefly skeletal muscle, and decreasing hepatic glucose production [102, 103]. Moreover, it has a role in the modulation of different other processes such as neurogenesis [104], cardiovascular diseases [105], cancer [106] and in the enhance of the lifespan of mice by increasing antioxidant protection and reducing chronic inflammation and oxidative damage [107].

Several studies have suggested that Metformin may operate on skeletal muscle stimulating glucose uptake independently of insulin, or acting on insulin binding protein or proximal components of the insulin signalling cascade [108]. In particular, the target of this drug is the AMP-activated protein kinase (AMPK) which become phosphorylated in a dose and time dependent manner inhibiting the mitochondrial respiratory chain complex and causing a decrease in ATP and increase in AMP concentration [103]. The consequence of AMPK activation is thus the enhance and translocation of

GLUT4 in muscle, fatty acid oxidation in muscle and liver and inhibition of triglyceride and cholesterol synthesis and lipogenesis [109].

Interesting is the role of Metformin on the inflammation. Phosphorylating AMPK, in fact, it ameliorates the anti-inflammatory activity decreasing the expression of mediators, such as TNFα, IL-1β, IL-6, nuclear factor κB (NFκB), fibrinogen, soluble vascular cell adhesion molecule-1, inducible nitric oxide synthase (iNOS) and cyclooxygenase (COX)-2 indicating to possess anti-inflammatory, anti-oxidative and anti-tissue remodelling properties [110].

AIMS

We aimed to study the origin of intermuscular fat and the complex mechanisms regulating the crosstalk with the surrounding muscle. We consider this of paramount importance in order to explain the pathophysiological aspects of obesity related sarcopenia which represents an important and emerging clinical issue. The project aims to investigate some characteristics of the pathology, by using both human samples and animal model. In particular we aimed:

- to understand the differences in muscle inflammation between obese patients, obese patients with type 2 diabetes and healthy subjects (that have not metabolic disorders), by collecting and analysing muscle biopsies;
- to verify the impact of weight loss, induced by bariatric surgery, on the release of muscle specific miRNA into blood circulation and to identify candidate miRNAs as potential useful markers of muscle inflammation in obese patients by using serum samples isolated from patients that underwent bariatric surgery.
- to investigate the role of ECM in the accumulation of intermuscular fat, by using a mouse model of obesity that display reduced muscle size and fiber and increased number of hybrid fibers (indicative of an earlier sarcopenic condition) [111]. Firstly, a decellularization protocol was set for quadriceps of wild type (wt) and obese (ob/ob) mice, then the decellularized samples were characterized in terms of DNA content and ECM structure preservation.
- to study the ability of the matrices to be remodelled and reabsorbed by performing transplantations of ECMs isolated from wt and ob/ob mice in wt mice model of volumetric muscle loss.

MATERIAL AND METHODS

3.1 Human

3.1.1 Human biopsies

Three human *rectus abdomins* biopsies from obese patients both normoglycemic and diabetic and three peroneal muscle biopsies from healthy subjects (that have not metabolic disorders) were collected by Bariatric Surgery Unit of Padua Hospital during Sleeve Gastrectomy surgery or by Padua Hospital Orthopaedic Unit during trauma surgery. All patients written inform consent for samples donation approved by Hospital Ethics Committee (N° 2892P- N°2682). Each sample was deprived of adipose and fibrotic tissues and frozen with cooled nitrogen.

3.1.2 Sera patients

Human sera patients were collected from 2012 to 2015 by Center for the Study and the Integrated Treatment of Obesity-Bariatric Unit at Padua Hospital. A cohort of patients that underwent bariatric surgery was selected; in particular sera of 24 obese normoglycemic, 17 obese diabetic and 6 healthy patients were analysed for principal myomiRNA levels. For each patient, 200ul of serum collected before and 1 year after surgery were evaluated (Table 1).

PATIENTS	NUMBER	SEX (M:F)	AGE	BMI
Normoglycemic	24	8:16	47±6	47±7
Diabetic	17	8:9	53±7	48±8
Healthy	6	3:3	28±3	20±1

Table 1: Classification and number of patients used for serum miRNAs analysis.

3.1.3 RNA extraction and quantification from human biopsies

Human muscle biopsies were put in 1ml of Qiazol (Qiagen) and homogenized mechanically for 3 minutes at 30Hz in a TissueLyser (Qiagen); then 200µl of chloroform were added and samples were mixed for 15 seconds. After 5 minutes at RT they were centrifuged at 4°C for 15 minutes at 12000g in order to separate the aqueous phase from the organic one. From the aqueous phase the RNA were extracted with Rneasy Plus Mini kit (Qiagen) according to the

manufacturer's instructions. From each samples 500ng of RNA were reverse-transcribed for 1 h at 37°C in a 50µl reaction containing 1X RT buffer, 150 ng random hexamers, 0.5 mmol/l dNTPs, 20 units of RNAsin Ribonuclease Inhibitor and 200 units of M-MLV RT (Promega Corporation, Madison, WI, USA). qPCR was carried out on StepOne Real time PCR system (Life Technologies) with Syber Select Master Mix (Applied Biosystems). Each cDNA was assayed in duplicate and standard curves were obtained using cDNA from human visceral adipose tissue by plotting values for log cDNA quantity (in AU) versus cycles threshold. For each sample, gene expression values were normalized by 18S content and reported as AU ratio. Genes analyzed and primers used in this work are reported in table 2.

human gene	**Primers sequences**
IL-1β	F: GGGCCTCAAGGAAAAGAATC
	R: TTCTGCTTGAGAGGTGCTGA
IL-6	F: TACCCCCAGGAGAAGATTCC
	R: TTTTCTGCCAGTGCCTCTTT
TNFα	F: GAACCCCGAGTGACAAGC
	R: TGGGAGTAGATGAGGTACAGG
TGFβ	F: AACAATTCCTGGCGATACCTC
	R: GTAGTGAACCCGTTGATGTCC

Table2: Sequences of human primers used in this work.

3.1.4 miRNA extraction and quantification from serum samples

All serum samples were put in 1ml of Qiazol (Qiagen),then 200µl of chloroform were added and samples were mixed for 15 seconds. After 5 minutes at RT they were centrifuged at 4°C for 15 minutes at 12000g in order to separate the aqueous phase from the organic one. From the aqueous phase the microRNAs were extracted with miRNeasy Serum/plasma kit (Qiagen) according to the manufacturer's instructions. 1,5µl of RNA template was retro transcribed for 1h at 37°C in 10µl of reaction containing 5x miScript Hispec Buffer, 10x miScript nucleic buffer, RNase free water and miScript Reverse Transcriptase mix (Qiagen). After that, 5µl of cDNA were pre-amplified for interested miRNA with miScript PreAmp kit (Qiagen). qPCR of miRNA 133a, miRNA 133b and miRNA 1 were carried out on StepOne Real time PCR system (Life Technologies) with miScript SYBR Green PCR Kit. Each cDNA was assayed in duplicate and standard curves were obtained using

cDNA from human muscle tissue by plotting values for log cDNA quantity (in AU) versus cycles threshold. For each sample, gene expression values were normalized by miR-RTC content and reported as AU ratio.

3.1.5 Statistical analysis

For statistical analysis, GraphPad Prism 6 software was used. Values are reported as means ± SEM. miRNA data set were compared by Kruskal-Wallis (ANOVA) non parametric test comparing all results with the control (α=0,05; *= p<0,5; **=p< 0,005; ***=p< 0,001;****=p < 0,0001).

3.2 Mouse

3.2.1 Animals

All surgical procedures and animal husbandry were carried out in accordance with University of Padua's Animal care and Use Committee (OPBA 413/2015-PR) and were communicated to the Ministry of Health and local authorities in accordance with Italian law. The animals used as donors (quadriceps muscles) were 4-5 month-old B6.Cg-Lep$^{ob/J}$male mice. These mice are homozygotes for a mutation in Leptin gene and are considered the most common model of obesity. They are characterized by hyperphagia, hyperglycemia, glucose intolerance, elevated plasma insulin, subfertility, impaired wound healing and an increase in hormone production from both pituitary and adrenal glands. They are also hypometabolic and hypothermic. Whereas as recipients, surgery controls and healthy control 4-5 month-old C57BL/6J male mice were used. All animals are bought from Jackson Laboratory.

3.2.2 Skeletal muscle decellularization

After mice sacrifice by cervical dislocation, wild type and ob/ob quadriceps were excised, cut in half and washed in sterile phosphate buffered saline 1X (PBS). The decellularization of samples was obtained using a detergent enzymatic treatment (DET), in which both chemical agents and enzymes were employed. Each DET cycle was composed of deionized water at 4 °C for 24 h, 4% sodium deoxycholate (Sigma-Aldrich) at room temperature (RT) for 4 h in gentle agitation, and 2000 kU DNase-I (Sigma-Aldrich) in 1 M NaCl

(Sigma-Aldrich) at RT for 3 h in gentle agitation (after a quick wash in PBS)(Fig.9). After decellularization, the matrices were preserved at 4 °C in PBS- 3% P/S (Gibclo-Life Technologies) for at least 3 days before their use or preserved in freezing medium (70% FBS (Gibclo-Life Technologies), 20% DMSO (Gibclo-Life Technologies), 10% DMEM high glucose (Gibclo-Life Technologies)) in liquid nitrogen. For wild type samples three DET were done, whereas for ob/ob quadriceps five DET were needed.

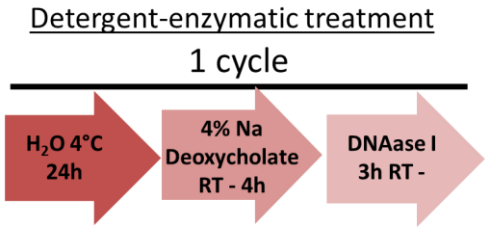

Fig. 9: Decellularization protocol used on wt and ob/ob quadriceps samples.

ECM characterization

3.2.3 DNA extraction and quantification

To assess total DNA content within the native quadriceps and decellularized matrices, samples were treated using DNeasy for blood&tissues kit (Qiagen). Up to 25 mg of tissues were first lysed overnight using proteinase K and buffer ATL . After lysis, 200 µl of absolute ethanol were added to provide optimal DNA binding conditions and the lysate was loaded onto the DNeasy Mini spin column. During centrifugation at 8000 rpm for 1 minute, DNA is selectively bound to the DNeasy membrane as contaminants pass through. Remaining contaminants and enzyme inhibitors are removed by washing with buffers AW1 and AW2. After the addition of each buffer ,tubes were centrifuged at 14000 rpm for 3 minutes. DNA was then prepared for elution by adding buffer AE, left to act for 10 minutes. Columns were then centrifuged at 8000 rpm for 1 minute in a new tube, in which nucleic acids were eluted. DNA extracts were evaluated using Nanodrop 2000 (Thermo scientific, USA). Nucleic acids have an absorption maximum at 260 nm. Most samples contain contaminates such as proteins and single stranded DNA/RNA that absorb maximally at 280 nm. Hence, optical densities at 260 nm and 280 nm were used to estimate the purity and yield of nucleic acids, which were quantified on the basis of 260 nm absorbance.

3.2.4 Immunofluorescence

Immunofluorescence for the analysis of the remaining nuclei into the decellularized ECM was done on samples fixed in 4% PFA for 1h at 4°C and then dehydrated at 4°C with a sucrose gradient method (10-15-30%). Then, matrices were included in the cryostat embedding medium O.C.T. (Kaltek) and frozen in isopentane (Sigma-Aldrich) cooled in liquid nitrogen, and subsequently processed using a cryostat (Leica) to produce 7 μm sections.

Sections on glass coverslip were then rinsed in PBS and permeabilized with Triton X-100 0.5% in PBS for 10 minutes at RT. Non-specific interactions were blocked with 10% HS in PBS for 12 minutes at RT. After washing, they were incubated with primary antibody rabbit anti-mouse Laminin (Sigma-Aldrich, dil. 1:100) for 60 minutes. Then, slides were washed and incubated with labeled secondary Alexa Fluor chicken anti-rabbit 488 (Invitrogen, dil. 1:200) for 1 hour at 37°C. Finally, nuclei were counterstained with fluorescent mounting medium plus 100 ng/ml 4',6-diamidino-2-phenylindole (DAPI) (Sigma-Aldrich). For each samples random pictures were collected with Leica DMI6000B microscopy and numbers of nuclei/field were counted.

3.2.5 Haematoxylin and eosin stain

Haematoxylin and eosin stain was done using Haematoxylin/Eosin (H-E) kit for rapid frozen section (Bio-Optica, UK).

Sections were rinsed in distilled water and put in reagent A (Harris haematoxylin) for 60 seconds and then rinsed in tap water. They were dipped in Buffer solution (prepared with reagent B) and rinsed again in tap water. Slides were put in reagent C (Eosin) for 37 seconds and dehydrated by dipping first in ethanol 95%, then in absolute ethanol and at the end in xylene; all dehydration steps were done twice. Sections were then mounted in organic mounting medium (Bio-Optica, UK).

3.2.6 Masson's trichrome stain

Masson's trichrome (MT) stain was done using Masson trichrome with aniline blue kit (Bio-Optica, UK). After a rapid hydration in distilled water, 10 drops of Weigert's iron haematoxylin A solution plus 10 drops of Weigert's

iron haematoxylin B solution were put on each section and left act for 10 minutes. Without washing, 10 drops of reagent C (Picric acid) were left to act 2 minutes on the sections. Slides were then rinsed in distilled water and incubated 1 minutes with 10 drops of reagent D (Ponceau's fuchsin) and rinsed again in distilled water. Subsequently, 10 drops of the reagent E were left on each section for 5 minutes, and without wash, 10 drops of the reagent F were left to act for 1 minute. After a final washing step in distilled water, section were dehydrated rapidly through ascending alcohols (50-75-95-100%). Sections were then cleared in xylene and mounted with organic mounting medium (Bio-Optica, UK). This histological procedure is able to identify different structures, such as the keratin and muscle fibers in red, collagen and bone in blue, cytoplasm in light red or pink, and in dark brown to black the cell nuclei.

3.2.7 Alcian blue stain

In Alcian blue (AB) stain, a sodium tetraborate solution transforms the dye into Monastral blue pigment, which is insoluble and can therefore be further manipulated without spreading in the tissue (Alcian blue-PAS). Alcian blue reacts with polyanions whose components are sulphuric and carboxylic radicals (phosphate radicals of nucleic acids do not react). As result, acid mucins only are stained. In particular, at pH 1 Alcian blue stains strongly sulphured mucins only, at pH 2.5 ionizes most acid mucins.

AB stain was done using Alcian blue pH 2.5 kit (Bio-Optica, UK). After a rapid re-hydration with descending alcohol gradient and distilled water, 10 drops of reagent A (Alcian blue pH 2.5) were left to act for 30 minutes on each section. Without wash, 10 drops of reagent B (sodium tetraborate) were put on each section and left to act 10 minutes. After a rinse in distilled water, section were incubated 10 minutes with 10 drops of reagent C (carmalum). After a final washing step in distilled water, section were dehydrated rapidly through ascending alcohols, stopping 1 minute in the last absolute ethanol. Sections were then cleared in xylene and mounted with organic mounting medium (Bio-Optica, UK).

3.2.8 Scanning Electron Microscopy (SEM)

Decellularized wt and ob/ob quadriceps for Scanning Electron Microscopy (SEM) were fixed for 24h in 4% paraformaldehyde (PFA) at 4°C. Following washing with PBS 1X, they were dehydrated in a gradient of ethanol (30-50-70-90-96-100%), dried using CO2 and finally mounted on aluminum stubs using sticky carbon taps. Samples were than coated with a thin layer of gold using Quorum (2m strumenti s.r.l) ion beam coater and images were captured with JEOL (JSM-6490) scanning electron microscope.

3.2.9 Collagen quantification

Collagen content of fresh and decellularized wt and ob/ob quadriceps mice was quantified using the SIRCOL collagen assay (Biocolor, UK) according to the manufacturer's instructions. Less than 25mg of fresh or decellularized samples were incubated overnight at 4 °C with 1 ml of 0.5 M acetic acid containing 0.1 mg of pepsin, to remove the terminal non-helical telopeptides and release the collagen into solution. Extracts were then incubated overnight at 4 °C with Acid Neutralising Reagent (contains TRIS-HCl and NaOH) and Collagen Isolation & Concentration Reagent (contains polyethylene glycol in a TRIS-HCl buffer, pH 7.6). After this step, samples were centrifuged at 12000 rpm for 10 minutes, supernatant was removed and samples were incubated 30 minutes in a mechanical shaker with Sirius red dye. Samples were centrifuged again at 12000 rpm for 10 minutes, supernatant was removed and Acid-Salt Wash Reagent (containing acetic acid, sodium chloride and surfactants) was added to remove unbound dye from the surface of the pellet and the inside surface of the micro-centrifuge tube. A final centrifugation step at 12000 rpm for 10 minutes was done and supernatant was removed. Alkali reagent (contains 0.5 M sodium hydroxide) was added and tubes were vortexed to release Sircol dye from the collagen-dye complex.

A volume of 200 µl of each sample was transferred into a 96 well microplate and Absorbance was determined at 555 nm with a microplate reader (Biorad). Reading was made at this absorbance because the spectrum chart

of the Sircol Dye in Alkali Reagent has a peak maximum in the visible region of 555 nm. Aliquots containing 0 - 6,5 - 12 - 25 and 50 µg of the Collagen Reference Standard (made of Collagen I extracted from bovine skin) were used to create a standard curve and determined collagen content.

3.2.10 Glycosaminoglycans quantification

The sulfated glycosaminoglycan (sGAG) content of fresh and decellularized wt and ob/ob quadriceps was quantified using the Blyscan GAG Assay Kit (Biocolor, UK). Less than 50mg of wet fresh or decellularized tissue was weighed and placed in a micro-centrifuge tube containing 1 ml of Papain Extraction Reagent: 0.2 M sodium phosphate buffer (Na_2HPO_4 – NaH_2PO_4) at pH 6.4, 0.1 M sodium acetate, 0.01 M Na_2EDTA, 0.005 M cysteine HCl, 15-20 mg of papain, and incubated in a water bath at 65 °C for 3 hours. Samples are then centrifuged at 10000 rpm for 10 minutes and supernatant was decanted off. Each sample was incubated for 30 minutes in a mechanical shaker with Blyscan dye (contains 1,9-dimethyl-methylene). Samples were centrifuged at 12000 rpm for 10 minutes, surnatant was carefully removed and dissociation reagent was added (contains the sodium salt of an anionic surfactant) to dissociate the sGAG-dye complex and enhance the spectrophotometric absorption profile of the free dye. A volume of 200 µl of each sample was transferred into a 96 well microplate and Absorbance at 656 nm was measured using a microplate reader (Biorad). A standard curve was set up using GAG standards containing 0 - 0,5 – 1 - 2 and 3µg of bovine tracheal chondroitin-4-sulfate, to determine the GAG content.

3.2.11 Elastin quantification

The Elastin content in fresh and decellularized wt and ob/ob quadriceps mice was quantified using the Fastin Elastin Assay Kit (Biocolor, UK). All test samples require the conversion of the native hydrophobic elastin into a water soluble derivative (α-elastin). To extract α-elastin, samples were heated at 100 °C for 1 h with 1 ml of 0.25 M oxalic acid twice. Samples were centrifuged at 10000 g for 10 minutes and surnatant was decanted off after each extraction period. Each sample was then incubated for 15 minutes with

ice cold Elastin Precipitating Reagent (containing trichloroacetic and hydrochloric acids). After a centrifuge at 10000g for 10 minutes, surnatant was removed and samples were incubated for 90 minutes in a mechanical shaker with Fastin Dye Reagent (contains 5,10,15,20-etraphenyl-21H,23H-porphine tetrasulfonate (TPPS) in a citrate-phosphate buffer). Samples were then centrifuged at 10000g for 10 minutes, surnatant was decanted off and Dye dissociation reagent (containing guanidine HCl and propan-1-ol) was added.

The contents of each tube was transferred into a well in a 96 well plate and Absorbance at 513 nm was measured using a microplate reader (Biorad). A standard curve was set up using standards containing 0 – 5 - 12.5 – 25 – 50 - 100 and 200μg of α-elastin from bovine neck ligament elastin, to determine the absolute elastin content.

***in-vivo* experiments**

3.2.12 Surgery procedure

For *in-vivo* transplantation, all ECMs obtained after decellularization protocol were washed in PBS 1X and sterilized with 0,1% peracetic acid for 1h at 4°C. Moreover, pH concentration was valuated before the implantation (pH=7).

Surgical procedures for creating VML on wild type mice were performed in general anesthesia (O_2 and Isofluorane, Merial, IT) by surgeon. A long incision on skin and muscle fascia of *tibialis anterior* (TA) was done and a critical size defect was created removing ~15mg of tissue. After the formation of the injury, ~ 15mg of wt or ob/ob ECM was implanted in the created pouch. The scaffold was sutured to the remaining TA muscle at middle and at the margins of the implant using prolene suture (6.0), muscle fascia and skin were sutured too and mice were reawaken (Fig.10).

	7 days	15 days	30 days
VML + wt ECM	n=2	n=2	n=2
VML + ob/ob ECM	n=2	n=2	n=2

Table 3: number of transplanted mice

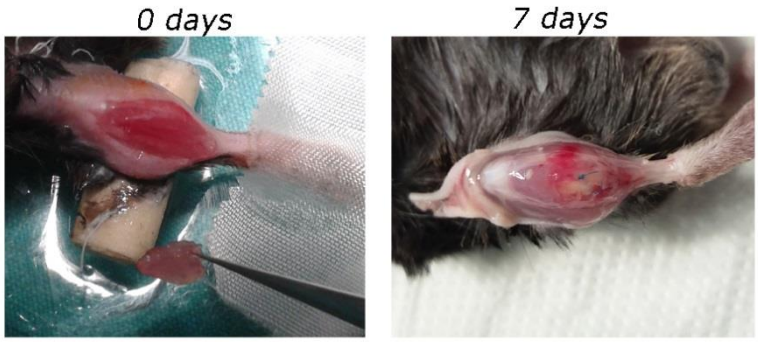

Fig. 10: Photos of VML damage creation and muscle condition after 7 days post-transplantation.

All animals survived to surgery and were sacrificed 7, 15 or 30 days after transplantation (table 3). Left TA muscles were frozen with cooled nitrogen for molecular analysis whereas right ones were fixed in 4% PFA and dehydrate in sucrose gradient for immunostaining.

3.2.13 Immunofluorescence

For immunofluorescence analysis on TA muscles obtained after VML and ECM implantation, sections of 7µm on glass coverslip were rinsed in PBS and permeabilized with Triton X-100 0.5% in PBS for 10 minutes at RT. Non-specific interactions were blocked with 10% HS in PBS for 12 minutes at RT. After washing, they were incubated with primary antibody for 60 minutes. Then, slides were washed and incubated with labeled secondary antibody for 1 hour at 37°C. Finally, nuclei were counterstained with fluorescent mounting medium plus 100 ng/ml 4',6-diamidino-2-phenylindole (DAPI) (Sigma-Aldrich). For these experiments the following primary antibody were used: rabbit anti-mouse ki67 (Abcam, dil. 1:100), rabbit anti-mouse Laminin (Sigma-Aldrich, dil. 1:100), rat anti-mouse Laminin (Santa Cruz Biotec., dil. 1:100), rat anti-mouse CD68 (Abcam, dil. 1:100). Whereas the secondary antibody used were: Alexa Fluor chicken anti-rabbit 594 (Life Technologies, dil. 1:200), Alexa Fluor chicken anti-rabbit 488 (Life Technologies, dil. 1:200), Alexa Fluor goat anti-rat 488 (Life Technologies, dil. 1:200), Alexa Fluor goat anti-rat 568 (Life Technologies, dil. 1:200). For each samples random pictures were collected.

3.2.14 Histological analysis

H&E stain, Masson's Trichrome stain and alcian blue stain were performed on slides of TA muscles obtained after VML and ECM implantation as previously described.

3.2.15 Real time PCR

After animal sacrifice, RNA of TA transplanted were extracted. All samples were put in 1ml of Qiazol (Qiagen) and homogenized mechanically for 3 minutes at 30Hz in a TissueLyser (Qiagen); then 200µl of chloroform were added and samples were mixed for 15 seconds. After 5 minutes at RT they were centrifuged at 4°C for 15 minutes at 12000g in order to separate the aqueous phase from the organic one. From the aqueous phase the RNA was extracted with Rneasy Plus Mini kit (Qiagen) according to the manufacturer's instructions. 2µg of RNA were treated with DNase treatment & Removal Reagents (Ambion, Inc, Austin, TX, USA) and reverse-transcribed for 1 h at 37°C in a 50µl reaction containing 1X RT buffer, 150 ng random hexamers, 0.5 mmol/l dNTPs, 20 units of RNAsin Ribonuclease Inhibitor and 200 units of M-MLV RT (Promega Corporation, Madison, WI, USA). qPCR was carried out on StepOne Real time PCR system (Life Technologies) with Syber Select Master Mix (Applied Biosystems). Each cDNA was assayed in duplicate and standard curves were obtained using cDNA from mouse quadriceps, visceral adipose tissue or spleen tissue by plotting values for log cDNA quantity (in AU) versus cycles threshold. For each sample, gene expression values were normalized by β2microglobulin content and reported as AU ratio. Genes analyzed and primers used in this work are reported in Table 3.

mouse gene	Primers
pax7	F: AGCAAGCCCAGACAGGTGGCG R: GGCACCGTGCTTCGGTCGCA
myf5	F: ACAGCAGCTTTGACAGCATC R: AAGCAATCCAAGCTGGACAC
myod	F: CGCTCAACTGCTCTTGATG R: TAGTAGGCGGTCTCGTAGCC
miogenin	F: GCAATGCACTCGAGTTCG R: ACGATGGACGTAAGGGAGTG
εMyHC	F: AGGCCTTGTGCTTTCCCAGAG R: GTTCACAGCATGGTGAACCTGG
AdipoQ	F: ACAATGGCACACCAGGCCGTGA R: AGCGGCTT TCCAGGCTCTCCTTT

IL-1β	F: ACGGACCCCAAAAGATGAAG R: CACGGGAAAGACACAGGTAG
TNFα	F: CTTCTGTCTACTGAACTTCGGG R: CAGGCTTGTCACTCGAATTTTG
INFγ	F: ACTGGCAAAAGGATGGTGAC R: TGAGCTCATTGAATGCTTGG
cebpb	F: CAAGCTGAGCGACGAGTACA R: AGCTGCTCCACCTTCTTCTG
nos2	F: GCAGGTCTTTGACGCTCGGA R: ATGGCCGACCTGATGTTGCC
arg1	F: AGACCACAGTCTGGCAGTTGG R: AGGTTGCCCATGCAGATTCCC
timp1	F: ATTCAAGGCTGTGGGAAATG R: CTCAGAGTACGCCAGGGAAC
mmp2	F: ACCTTGACCAGAACACCATC R: TCGCTCCATACTTTTAAGGCC
mmp9	F: AACTCACACGACATCTTCCAG R: CTGCACGGTTGAAGCAAAG

Table3: Sequences of mouse primers used in this work.

3.2.16 Statistical analysis

For statistical analysis, GraphPad Prism 6 software was used. Values are reported as means ± SEM. Data set were compared by non-parametric ANOVA with multiple comparisons (α=0,05; *= p<0,5; **=p< 0,005; ***=p< 0,001;****=p < 0,0001).

RESULTS

4.1 Human

Recently, literature articles suppose a possible correlation between inflammatory condition and increased presence of microRNAs in body fluids. Up to now, all published works were focused on dystrophies in which the progressive muscle loss was induced mainly by genetic mutations. In this study, instead, we considered a disease which is the result of a metabolic syndrome and in particular we focused on patients that, after an educational training, underwent bariatric surgery. From these subjects, both muscle biopsies and serum samples were collected: the first were analysed for selected inflammation markers, whereas the second for the principal muscle miRNAs (Fig.11).

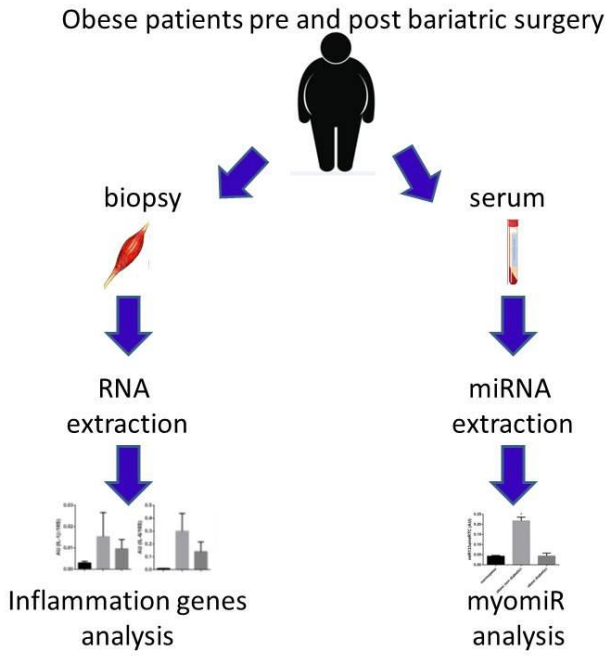

Fig. 11: Experimental plan for human samples.

Preliminary results obtained by real-time PCR on mRNA from muscle biopsies seemed to indicate that the muscle of normoglycemic obese subjects was more inflamed than healthy and diabetic obese patients even if no statistical differences were observed. According to what we know about adipose tissue inflammation correlating to obesity we could observe an increase in pro-inflammatory genes both in normoglycemic and diabetic

patients in comparison with the controls. However, in contrast to what we expected, diabetic subjects showed an inflamed reduction probably due to Metformina therapy which these subjects were submitted for diabetic treatment (Fig.12).

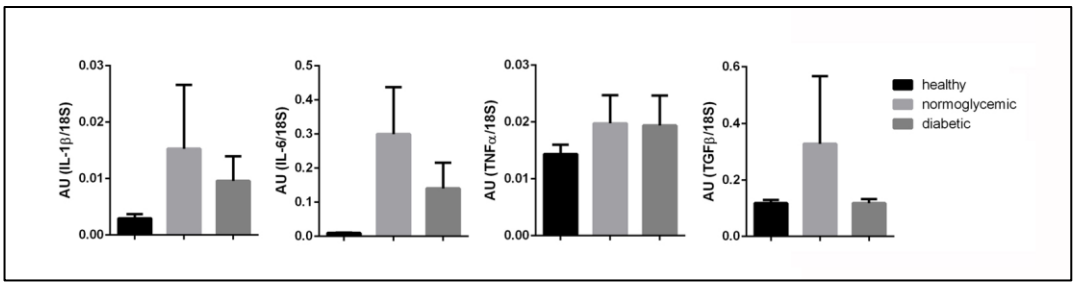

Fig. 12: Inflammatory genes (*IL-1β, IL6, TNFα, TGFβ)* analysed on muscle biopsies (n=3 for each group analysed).

With the aim to understand which was the involvement of surgery on skeletal muscle inflammation and to find an easy predictive marker useful to study the atrophy and muscle condition of obese subjects, the principal muscle miRNAs were analysed on serum samples collected before and one year after sleeve gastrectomy. What we showed was that surgery, which induced a decline of body weight, did not impair muscle condition. No quantity differences, in fact, were observed among groups for all the analysed miRNAs (Fig. 13). For this reason further analyses were done only on sera collected before surgery.

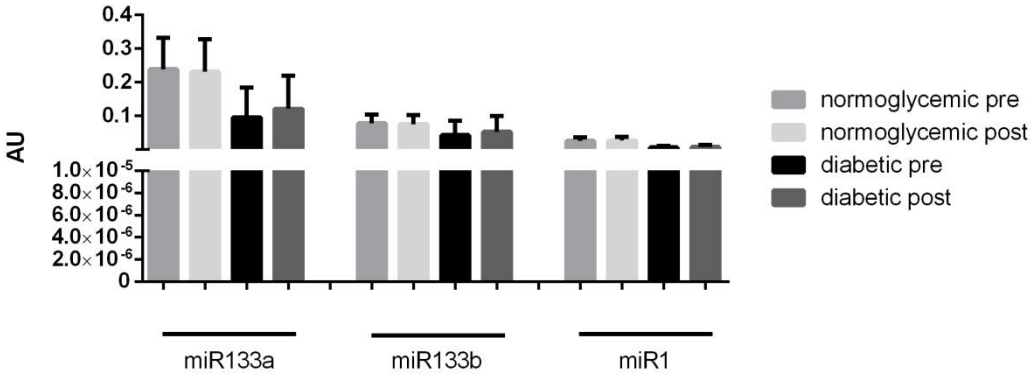

Fig 13: Differences on miRNA quantification obtained comparing serum samples collected before (pre) and after 1 year (post) bariatric surgery.

Results obtained on serum samples were similar to those of tissues. Indeed we observed an increase of miR133a, 133b and miR1 in normoglycemic patients compared to healthy and diabetics (Fig.14).

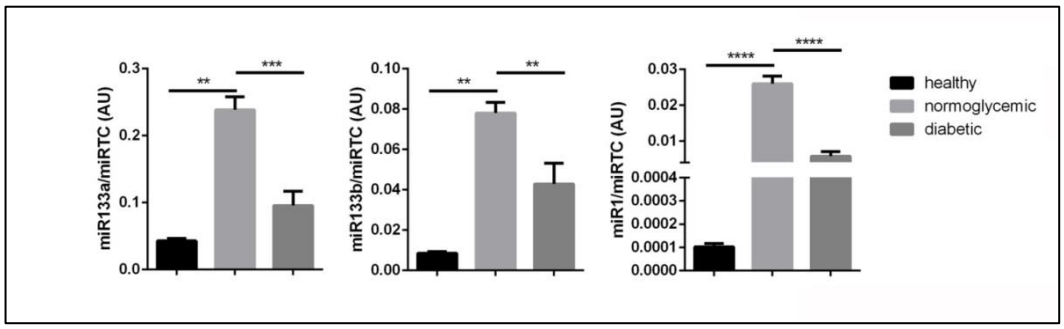

Fig. 14: Results obtained on miR133a-miR133b and miR1 quantification on serum sample of healthy, normoglycemic obese and diabetic obese patients (**=p< 0,005; ***=p< 0,001;****=p < 0,0001).

4.2 Mouse

With the aim to investigate the role of the extracellular matrix into the onset of pathophysiological conditions such as sarcopenic obesity, a specific mouse model was used. B6.Cg-Lep$^{ob/J}$ (ob/ob) mice are genetically engineered to not express Leptin thus to mimic human obesity; they display size and fiber reduction and a shift in their fibre type composition towards a slower, more aerobic-oxidative phenotype as seen in the first sarcopenic stages [111]. For these reasons they were considered useful to study the adverse mechanism affecting muscle stem cells and their microenvironment during this pathological condition. In particular, in this study, quadriceps muscles from wild type (wt) and ob/ob mice were collected, decellularized and analysed for structural components preservation and then implanted in vivo to study the extracellular matrix ability to be remodelled and reabsorbed (Fig. 15).

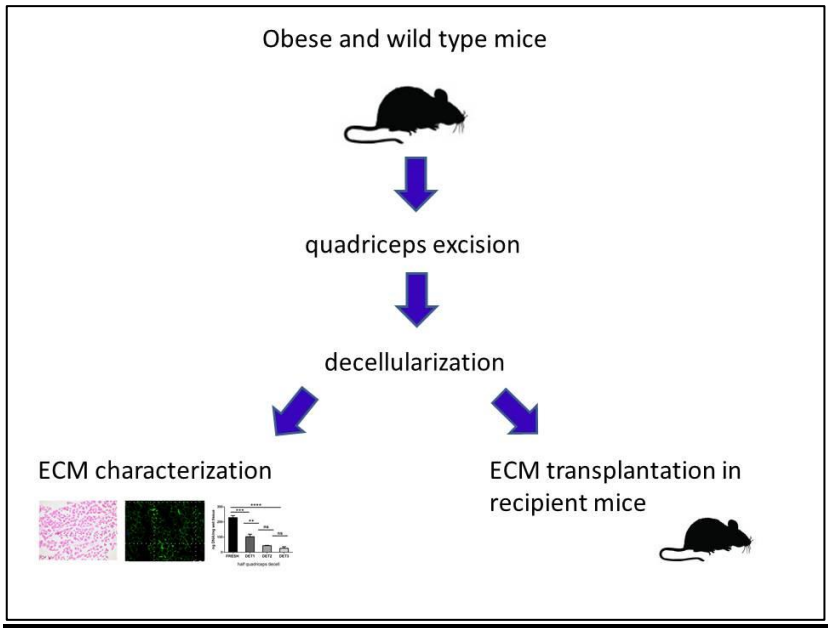

Fig.15: Experimental plan for mouse samples.

4.2.1 Decellularization efficiency and characterization of ECM components

The decellularization treatment used in this work was previously described for other organs [112] and was a cyclic combination of the detergent solution NaDeoxycholate, which widened the mesh of the matrix, and the enzyme DNAase I which degraded genomic components. First of all, we defined the number of cycles needed to obtain the greatest removal of cellular compartment preserving structural properties.

Wild type sample sections stained for laminin and DAPI were used to evaluate microscopically both fibre structure and presence of cells (nuclei). Counting the number of nuclei *per* field in 5 random pictures of fresh (178±8 nuclei/field) and decellularized sample slides (DET3: 27±25 nuclei/field), it was demonstrated that the decellularization process rapidly decreased the cellular compartment of the muscle, obtaining a quite complete nuclei depletion after 3 cycles. These data were also evaluated by the quantification of DNA content (fresh: 228±27; DET1: 103±40; DET2: 44±6; DET3: 31±22 ng/mg wet tissue) which showed a reduction of 87% of DNA after 3 cycles of decellularization compared to fresh quadriceps.

Ob/ob muscles, instead, were more compact than the wild type control, reflecting the muscle atrophy characteristics of a sarcopenic-obesity

condition. This was demonstrated by the need to improve the number of decellularization cycles to obtain the same genomic reduction. Only after five cycles of decellularization, in fact, we were able to obtain a significant nuclei/field and DNA content reduction (Fresh: 259±24; DET5: 31±6 nuclei/field; Fresh: 371±191; DET3: 139±26; DET4: 105±7; DET5: 73±19 ng/mg wet tissue) with 81% loss of genomic component (Fig. 16A). At SEM analysis we observed that in both decellularized matrices the fiber structure was preserved and lacking of nuclei (indicating by holes on fibers).

In order to characterize the components and to evaluate the differences between wt and ob/ob matrix structure obtained after decellularization protocol, a quantitative assays for GAGs, elastin and collagen components were performed. These analyses showed a significant reduction on decellularized samples in comparison with the respectively fresh quadriceps but no differences were noted when comparing decellularized samples between groups. In particular, for GAG, a long unbranched polysaccharides that consist of repeating sugar dimers with diverse and numerous roles in connective tissues, there was a statistical reduction content on wt decellularized samples in comparison with fresh wt quadriceps (fresh: 0,2229 ± 0,05974; DET3: 0,02891 ± 0,007921 µg/mg wet tissue). Whereas, for ob/ob samples no differences were demonstrated (fresh: 0,1443 ± 0,07627; DET5: 0,06368 ± 0,02026 µg/mg wet tissue).

Elastin, which provides the necessary elasticity to the tissue, seemed to be decreased after decellularization both in wt and ob/ob quadriceps but no difference was observed when comparing the acellular muscles (fresh wt: 19814 ± 2263; DET3 wt: 858,4 ± 1397; fresh ob/ob: 17149± 1030; DET5 ob/ob: 3957 ± 2192 µg/mg wet tissue).

Finally, differently from other components, collagen was preserved after decellularization both in wt and ob/ob ECM (fresh wt: 836,9 ± 555,5; DET3 wt: 331,1 ± 195,6; fresh ob/ob: 791,4 ± 689,3; DET5 ob/ob: 177,5 ± 35,78 µg/mg wet tissue) (Fig. 16B).

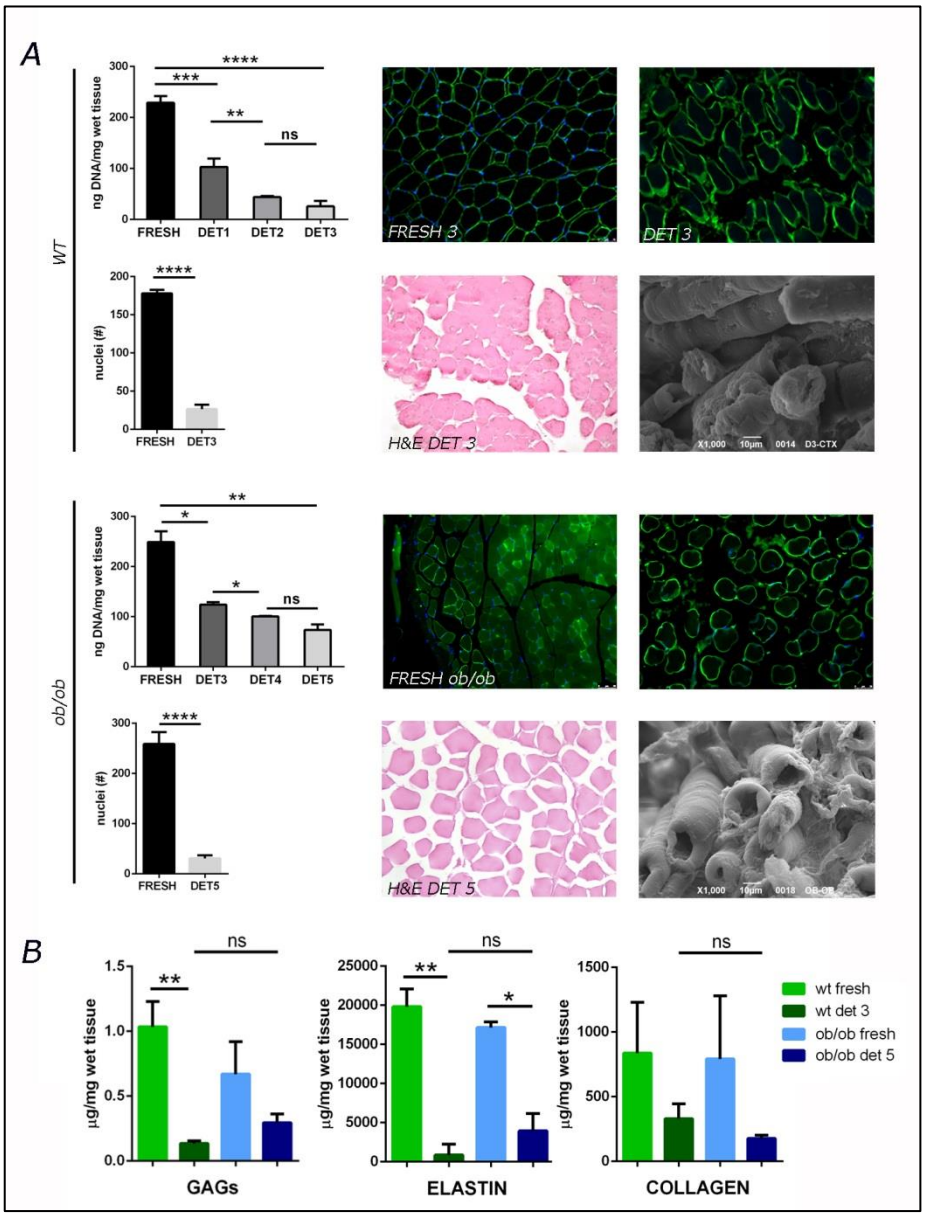

Fig. 16: Decellularization efficiency and characterization of ECM components. A) Quantification of DNA content and number of nuclei/field remaining after decellularization protocol on wt and ob/ob quadriceps. Immunofluorescence analysis, H&E staining and SEM observation on fresh and DET3 (for wt samples) and DET5 (for ob/ob samples) demonstrating macroscopically the greatest removal of cellular compartment and preserved structure. B) GAGs, Elastin and Collagen quantification on fresh and decellularized samples. (*= p<0,5; **=p< 0,005; ***=p< 0,001;****=p < 0,0001).

4.2.2 In vivo experiments

All wt animals survived after surgery without signs of infection and implant rejection. After 7, 15 and 30 days animals were sacrificed and the *tibialis anterior* muscles (TA) were exceeded and analysed to study the matrix remodelling and the signals released by obese mouse's matrix into a healthy recipient. At first, we investigated the presence of the implanted matrix, its reabsorption and cells infiltration. At all time points, matrix implantation was noticeable thanks to its different fiber orientation or to the proximity of the stitches; however it was easier in 7 days samples than at 15 and 30 days sections.

In order to investigate the contribution of donor implantation to the deposition of the principal matrix structures, sample sections were analysed with different histological stains at each time point. After 7 days both wt and ob/ob extracellular matrix (ECM) induced a strong cells migration in the interface between native tissue and matrix that gradually diminished after 15 and 30 days. In addition, Alcian blue and Masson's Trichrome stains highlighted no differences between groups in the deposition of GAG and collagen components when comparing the same time points and different donor matrices. In particular we observed that the matrices derived from donor affected by a metabolically disease did no induce an alteration in structural matrix deposition (Fig.17).

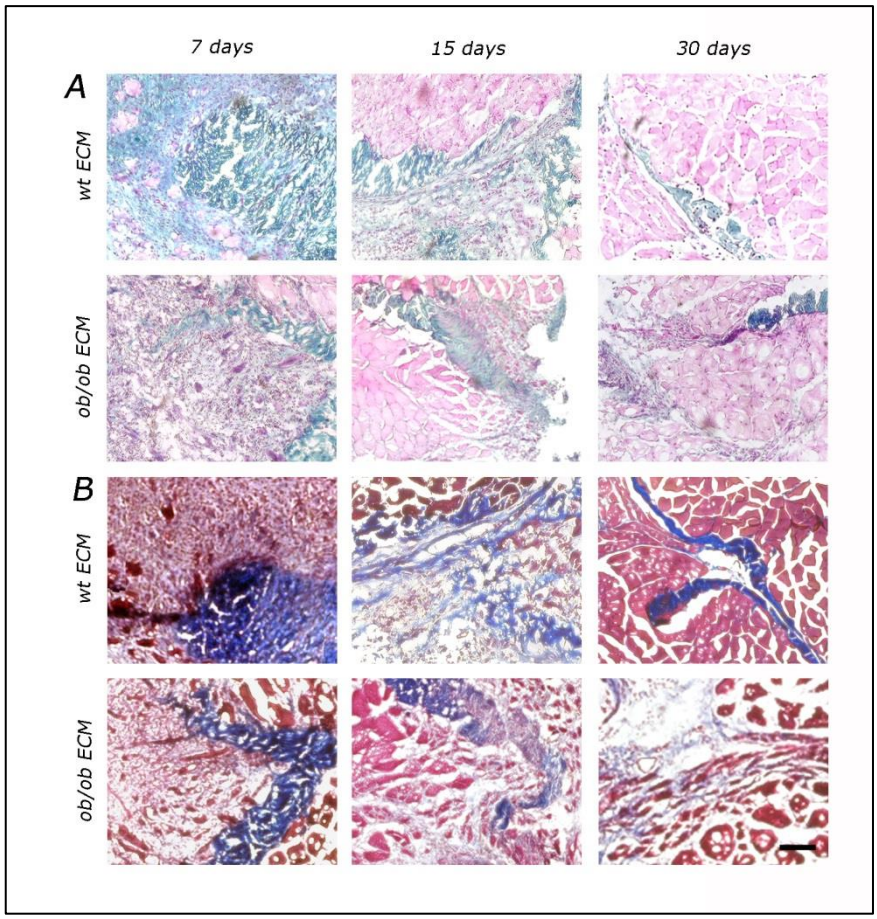

Fig. 17: Alcian Blue (A) and Masson's trichrome stain (B) on sections of wt TA after 7, 15 and 30 days of volumetric muscle loss and different ECM implantation . (Scale bar=300µm).

As we expected, at 7 days by immunofluorescence analyses we observed a greater number of ki67 positive proliferating cells (7 days wt ECM: 10,17 ± 1,926; 7days ob/ob ECM: 5,190 ± 1,160 % positive cells) indicating tissue regenerating process according to the physiological response after injury. This cells activation was progressively reduced overtime in both samples implanted with wt and ob/ob decellularized matrices. However, no statistical differences were observed analysing wt or ob/ob ECM (15days wt ECM: 5,017 ± 3,590; 15 days ob/ob ECM: 2,920 ± 2,644; 30days wt ECM: 0,2000 ± 0,2828; 30days ob/ob ECM: 0,4200 ± 0,1131; 30days sham: 0,5000 ± 0,7071 % positive cells). Results obtained after 30 days post implantation were always compared to sham experiment in which the same exceeded TA portion was then re-implanted. Also in this case there were no differences among groups (Fig. 18).

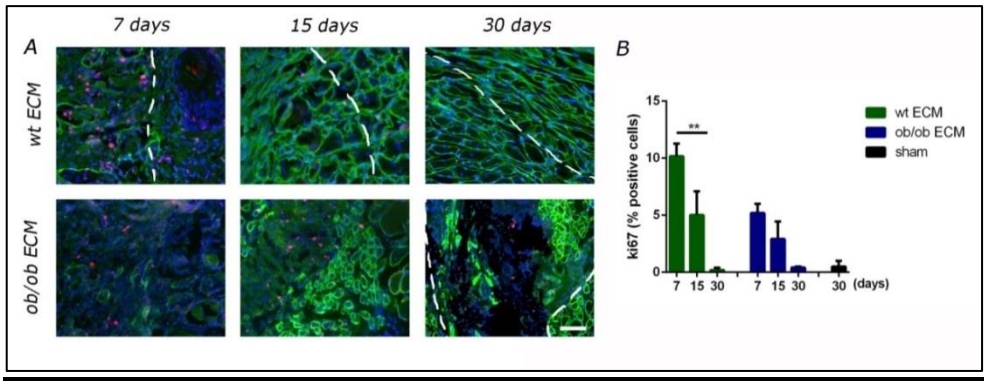

Fig. 18: A) Immunofluorescence analysis for ki67 markers on wt TA samples obtained after volumetric muscle loss and different ECM implantation (scale bar 300µm); B) Quantification of ki67 positive cells (%) present on TA after 7,15 and 30 days post-transplant.

To understand if there was a contribution of the matrices to muscle inflammation, TA slide sections were stained for CD68 marker, which identify macrophages infiltration. $CD68^{+}$ cells were found in ECM implantation, mainly in the area around the stitches and in the interface between the matrix and the native tissue (Fig. 19, Fig. 20, Fig. 21). Counting the number of CD68 positive cells *per* field in 5 random pictures of each sample, ob/ob ECM seemed to chemoattract more macrophages after 7 days in comparison with wt ECM (7 day wt ECM: 24,84 ± 3,749; 7 days ob/ob ECM: 42,73 ± 11,52 % positive cells) even if there were no statistical differences among groups for all time points (15 days wt ECM: 31,18 ± 13,73; 15 days ob/ob ECM: 20,93 ± 2,901; 30 days wt ECM: 28,52 ± 20,95; 30 days ob/ob ECM: 17,97 ± 4,561; 30 days sham: 11,49 ± 2,251 % positive cells)(Fig.22). Furthermore, no immune response was detected in the native TA as a consequence of transplantation, since no inflammatory infiltrate and no signs of damage caused by inflammatory response were detected at any time point.

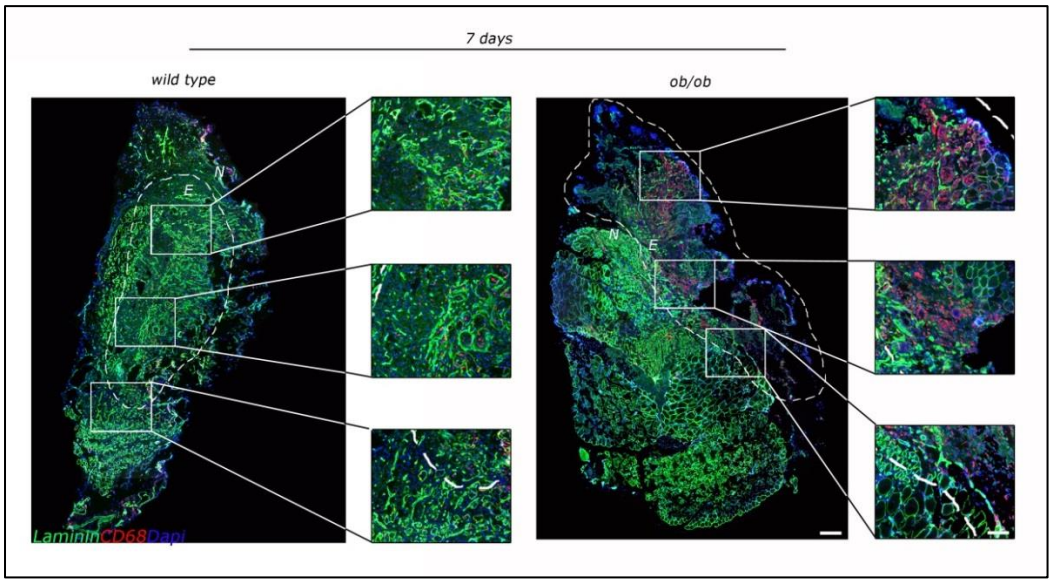

Fig. 19: Immunofluorescence CD68 stain on 7 days section slides (scale bar 100µm) with magnification of transplanted ECM (scale bar 300µm).

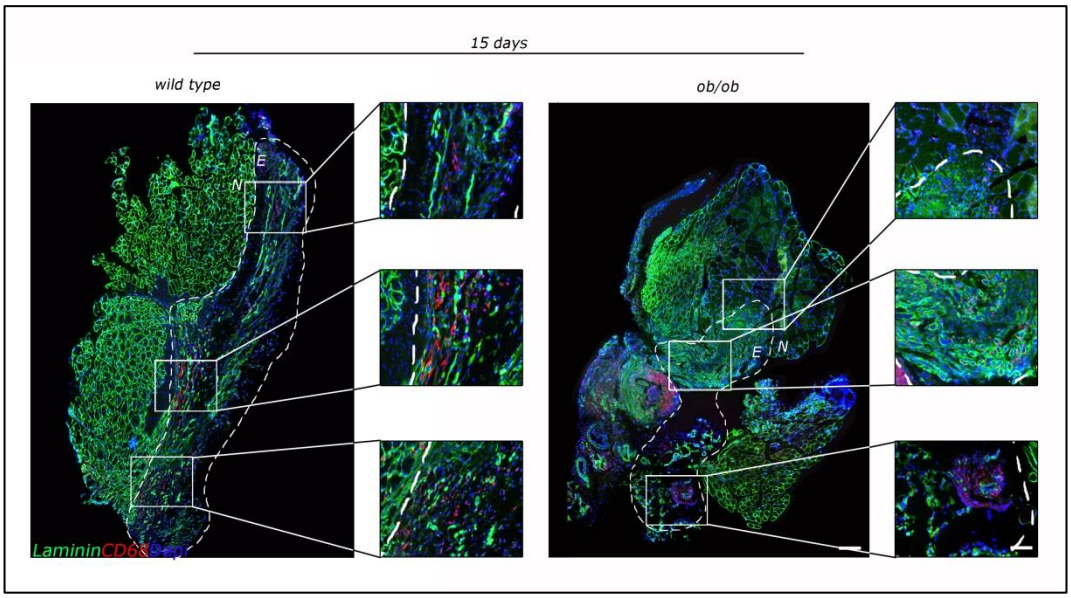

Fig. 20: Immunofluorescence CD68 stain on 15 days section slides (scale bar 100µm) with magnification of transplanted ECM (scale bar 300µm).

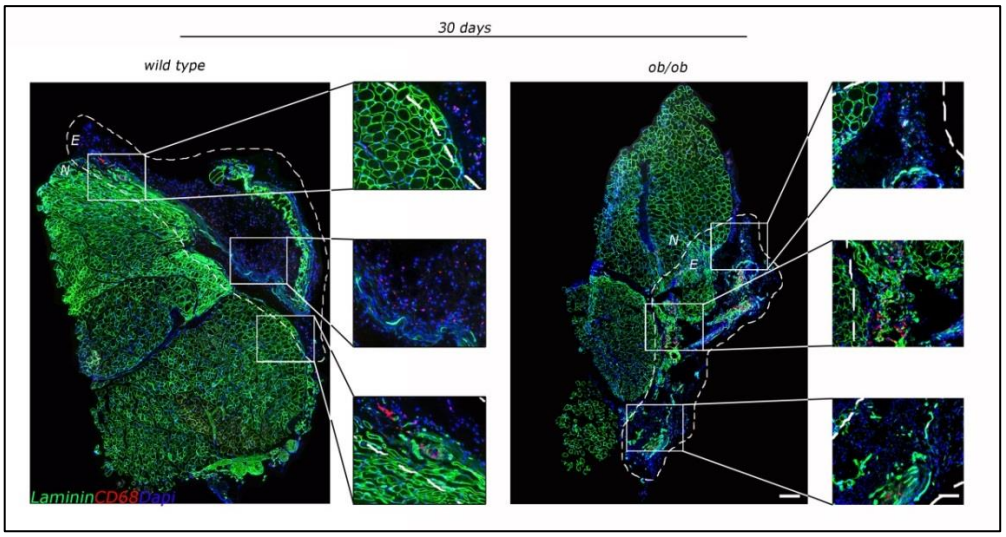

Fig. 21: immunofluorescence CD68 stain on 30 days slides (scale bar 100µm) with magnification of transplanted ECM (scale bar 300µm).

We also performed a real-time PCR to determine which types of macrophages were more involved analysing *Nos2* and *Arg1* expressions as M1 and M2 markers respectively. While there were no differences among groups on Nos2 levels, a significant variation was observed in Arg1 expression. In particular wild type samples induced a progressive attraction of inflammatory cells which was lower at 7 days and greater at 30 day ($p<0,5$), whereas ob/ob matrices promoted exactly the opposite behaviour with greater M2 activation at 7 days (Fig.22).

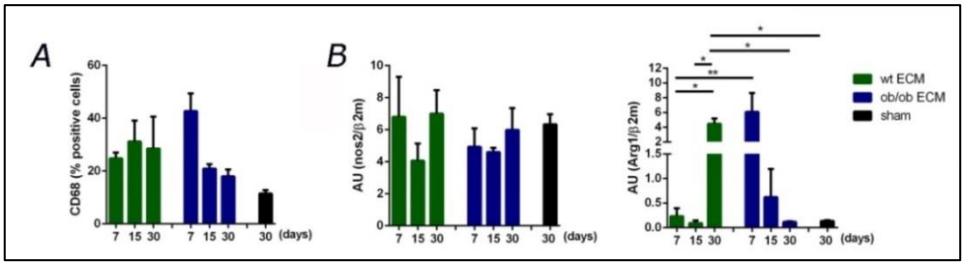

Fig. 22: A) Quantification of CD68 positive cells (%) present on TA after 7,15 and 30 days post-transplant. B) Results obtain by real time PCR for *nos2* and *Arg1* genes, marker of M1 and M2 macrophages respectively (*= $p<0,5$; **=$p< 0,005$).

Given the knowledge that macrophages were responsible for inflammation resolution by producing high levels of matrix remodelling factors (MMPs, TIMPs), we decided to investigate these elements in association with some

pro-inflammatory genes. For *IL-1β, TNFα* and *mmp2* we observed an opposite behaviour between wild type ECM and ob/ob ECM. Furthermore, in our samples, we showed this increased *mmp9* level after 7 days post implantation, indicating an early remodelling of the matrix which was reduced in the longer time points (Fig.23, Fig.24). Also in this case, similarly to *Arg1*, it seemed that matrices derived from obese mice were able to induce a premature inflammation response that reduced or stabilised after 30 days. On the contrary, the implantation of an healthy matrix needed more time to start a remodelling response albeit leading to a probable better and complete damage resolution.

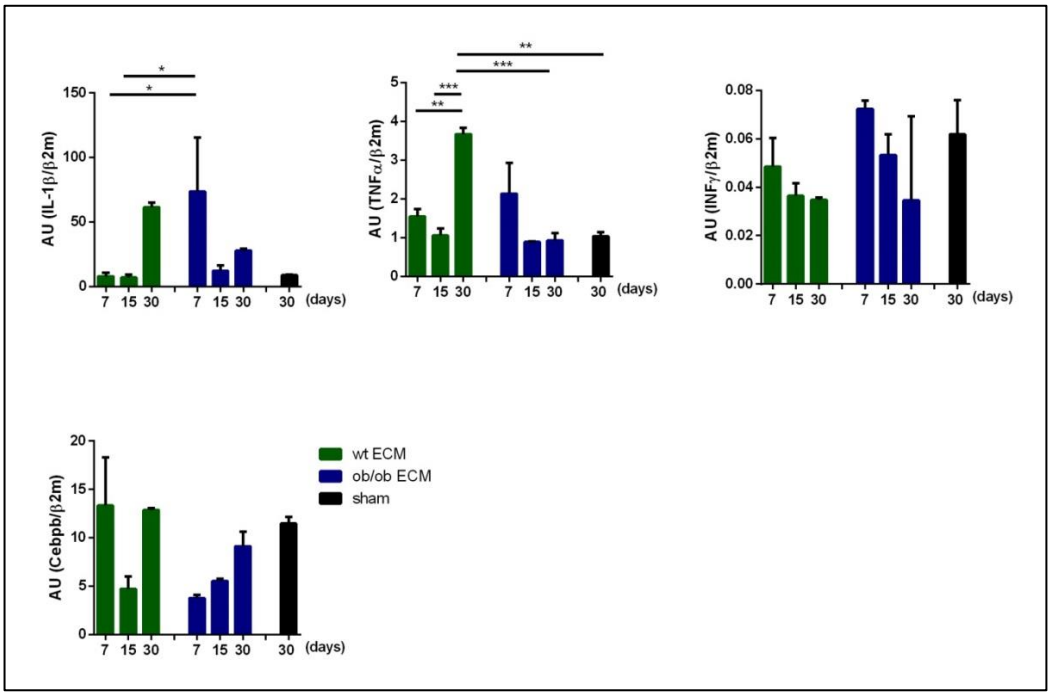

Fig. 23: mRNA expression level of *IL-1β, TNFα, INFγ* and *Cebpb* analysed by real time PCR to understand the level of inflammation induced by the presence of the different matrices on transplanted TA (*IL-1β, TNFα, INFγ* are the most important pro-inflammatory gene, whereas *Cebpb* was analysed for its significant role in adipogenesis) (*= p<0,5; **=p< 0,005; ***=p< 0,001).

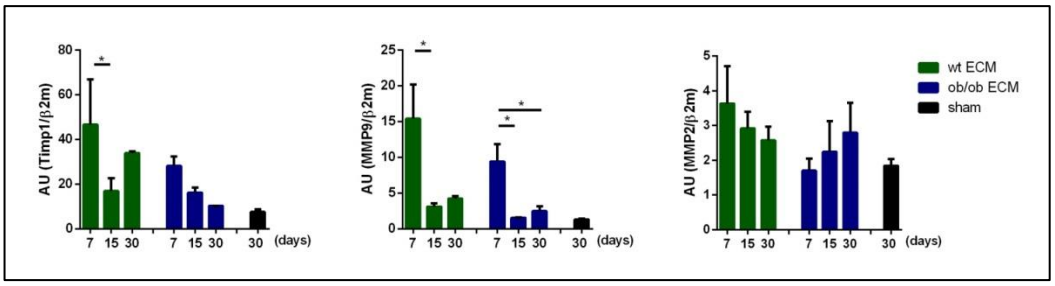

Fig. 24: real time PCR for principal ECM remodelling factors, such as *Timp1* (inhibitor of metalloproteases), *MMP9* and *MMP2* (metalloproteases involved in the cleavage of collagen) on transplanted TA (*= p<0,5)

In conclusion, since no structural or inflammation differences were observed, we focused on cellular signalling modification. mRNA from TA of all animals was extracted and the main myogenic markers were analysed in order to verify if different donor ECM altered the myogenic pathways. What we noticed was that there were some differences in cells activation between the wt ECM (earlier myogenic cell activation program) and the ob/ob ECM (later cell activation). However for all analysed genes there were no significant differences.

We also analysed *AdipoQ* gene in order to investigate if the ob/ob matrix could induce a switch of muscle stem cells into adipogenic commitment but in this case as well no differences were observed even in comparison to the sham (Fig. 25).

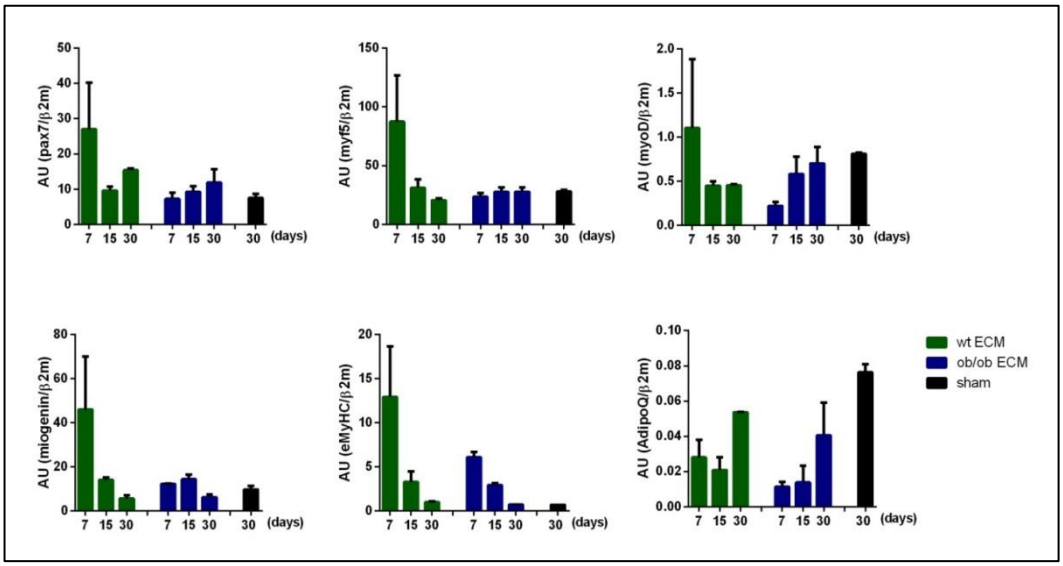

Fig. 25: Real-time PCR for principal myogenic and adipogenic markers on TA samples. In particular mRNA expression levels of *pax7, myf5, myod, miogenin and eMyHC* were analysed to evaluate potential

myogenic changes and *AdipoQ* gene as marker of possible activation of adipogenic signaling on transplanted TA.

DISCUSSION

Obesity is a complex multifactor disease defined as an excess of body adiposity able to greatly increase the risk to develop several comorbidities like type 2 diabetes, cardiovascular diseases, disability and cancer. It arises when the balance between caloric intake and consumption is lost and brings to an excess fuel substrates deposition in adipose tissue. Hereditary genetic factors, family circumstances, ethnic differences, age but especially socio-economic and socio-cultural conditions that support sedentary and unhealthy lifestyle, are some of the prognostic factors leading to this pathological condition, which is reaching epidemic proportions.

Up to now, obesity was considered only as a quantitative trait and nosographycally classified using the Body Max Index (BMI). However, also waist circumference, which is strongly correlated to the amount of dangerous and metabolically active visceral adipose tissue, has recently become an increasing discriminating measure. [113]

Aging is another relevant aspect that is often associated to higher predisposition to increase of body weight and visceral adiposity and it is also correlate to a great muscle volume and strength loss (sarcopenia), which dramatically reduce life quality. The coexistence of aging and obesity is named sarcopenic obesity and has worst effects than the two single diseases.

In obese patients, a cross-talk between dysfunctional adipose tissue and skeletal muscle is widely described. By definition, in obesity, adipose tissue is characterised by hypertrophy and hyperplasia that allow to have an increased flux of lipid substrates to be stored. This physiological function could be lost after the development of cell insulin resistance, the presence of macrophages infiltration, tissue inflammation and altered adipokine secretion. All of these aspects result in an insufficient ability of the tissue to further expand itself and to store lipids. Therefore, this excess of fatty acids is accumulated also in several other organs, including skeletal muscle, where induces metabolic dysfunctions, β-oxidative alterations, increase of ROS production, lipotoxicity and insulin resistance. Moreover, this intermuscular adipose tissue (IMAT) acts as chemoattractant for inflammatory cells, chiefly

macrophages, which produce high amount of pro-inflammatory cytokines contributing to both local and systemic inflammation.

Although several works correlate the amount of intermuscular adipose tissue and related inflammation with quantitative and qualitative muscle alterations, little is known about the molecular aspects that induce muscle loss and strength impairments that characterize sarcopenic obesity; even less are the studies performed in humans.

The strength of this work lies in the use, for a part of the analysis, of human muscle biopsies and sera from healthy and obese patients both normoglycemic and diabetic who underwent to bariatric (obese subjects) or orthopaedic surgery (healthy subjects).

On this first pilot study, analysing the most important genes encoding for inflammatory proteins, we observed that there was a greater muscle inflammation in biopsies of obese patients in comparison with healthy subjects. Despite these findings are in keeping with other studies, surprisingly we noticed that the muscles from diabetic patients were less inflamed that the tissues collected from the normoglycemic subjects. It was not so simple to find an adequate explanation for this result and only comparing patient medical records we observed that all diabetic subjects were treated with Metformin from at least 1 year.

Metformin is a pleiotropic drug mainly used for the treatment of type 2 diabetes thanks to its effect on liver glucose metabolism, but recent studies have also demonstrated its possible role on inflammatory reduction in muscle cell lines and murine models. In particular, acting directly on AMP-activated protein kinase (AMPK) phosphorylation it seems to be able to reduce the expression of inflammatory factors like TNFα, IL-1β, IL-6 in macrophages, microglia, astrocytes, and mesangial cells [114]. Other works instead have showed a direct role of Metformin to NFκB inhibition, NO production and ROS reduction in endothelial cells and human adipocytes [103]. However, until now, nobody has investigated the role of Metformin on the inflammatory reduction in human skeletal muscle. For this reason our results could represent a preliminary proof, which needs to be further

investigated in a larger population, that Metformin treatment could have an additional beneficial effects on muscle of obese diabetic people.

Since several papers have demonstrated the role of microRNA both in physiological and pathological processes, we decided to correlate our results with some miRNA associated to skeletal muscle and released in the blood circulation. Observing the levels of miR133a, miR133b and miR1 in the sera samples of a cohort of healthy and obese patients both normoglycemic and diabetic, we noted the same trend previously described for muscle biopsies. This suggests a possible direct correlation between muscle inflammation and the release of these circulating miRNA, which could be used in the future as indicative markers of patient muscle alterations.

As we previously described, the systemic inflammatory condition of obese patients derived mainly from the increase of adipose tissue in ectopic districts. Because it is well known that in chronic diseases, as obesity and diabetes, multifactorial components contribute to the pathology, we decided to investigate also the microenvironment of skeletal muscle, in term of extracellular matrix composition and biological activity, in order to understand if it could have had a role in the deposition of intermuscular adipose tissue and on associated inflammatory processes. To do that, we used a genetically engineered mouse model that mimics obesity and, using our knowledge on decellularization of tissue and organs [112], we investigated the matrix composition and its ability to be *in vivo* remodelled.

At first, we set a detergent enzymatic decellularization protocol on quadriceps of wild type (wt) and obese (ob/ob) mice which combined cyclical NaDeoxycholate and DNase I actions to remove genomic components preserving 3D matrices structures. Although for ob/ob samples we needed to improve the decellularization cycles to obtained the same results of wt quadriceps, we observed a macroscopical (indicated by immunofluorescenze analysis, H&E stain and SEM observation) and structural composition similarity (indicate by GAGs, elastin and collagen assays) between the samples.

At present, several regenerative medicine approaches are used to recover muscle damages. The most promising are those who use acellular scaffold

with or without stem cells and that are able to release factors favouring muscle improvement. In our case, starting from structure similarities between the two matrices, we decided to use a volume muscle loss model to investigate *in-vivo* if the matrix derived from a metabolically altered donor could be able to induce a different regenerative processes in comparison with the healthy one. In particular, a critical size defect was created on *tibialis anterior* of wild type mice, and wt ECM or ob/ob ECM were implanted in the injuries. After 7, 15 and 30 days muscles were exceeded and analyzed for ECM remodeling, inflammatory cells activation and for myogenic and adipogenic pathways modulation in resident cells.

From these analysis we observed that in all transplanted animals there were no inflammation or damages in native tissue and that both matrices were reabsorbed and remodelled. In particular, both wt and ob/ob ECM induced a strong cells migration on the interface between native and patch tissues stimulating a physiological response to the injury (see immunofluorescence stain and quantification of ki67 positive cells). Moreover, we did not observe differences in GAGs and Collagen deposition indicating that ob/ob matrix was not able to stimulate a greater fibrotic deposition in comparison with wt ECM.

After a transplantation of a tissue engineering scaffold or a biomedical device, the induced immune response depends on different factors including the material of the implant and its physical and mechanical properties. However, one aspect is always in common, the main role of innate and adaptative macrophages response. In regenerative medicine, where the acellular scaffold is used also as delivery of biochemical signals, the first stimulated response is the monocytes migration and pro-inflammatory cytokines release (TNFα, IL-1β). Depending on the nature of the stimuli, monocytes are activated and they can differentiate in macrophages with different phenotype. M1 macrophages, that exhibit a pro-inflammatory profile displayed during the early stages of regenerative process, whereas M2 macrophages are associated to the later stages and have an anti-inflammatory action. M2 subtype is also able to release angiogenic factors and promote ECM components production [115, 116].

Starting from these prerequisites, we investigated also in our samples the inflammatory response (CD68 positive cells). Even though there were no signs of implant rejection, $CD68^+$ cells were observed in the interface between native tissue and implanted ECM. No differences were noted in the quantity of these cells even if ob/ob ECM seemed to induce a slightly higher macrophages activation after 7 days compared to wt ECM. Using Nos2 expression as M1 macrophages marker and Arg1 expression for M2 subtype we investigated which type of polarization was stimulated in our samples. While no differences were observed for Nos2 level between groups, Arg1 had exactly opposite behaviour. In particular, wt ECM induced a strong macrophages polarization to M2 phenotype only after 30 days post implantation, whereas ob/ob ECM showed a strong presence of M2 macrophages at 7 days but after 30 days they were almost absent. Despite these differences not being significant, our hypothesis is that wt ECM is able to induce a physiological regenerative process that requires more time to move from a foreign body response to a positive remodelling process, whereas ob/ob matrix triggers immediately a strong remodelling which is soon stopped and that it probably does not lead to a complete resolution of the damage. Also for some inflammatory and matrix remodelling genes (*IL-1β, TNFα* and *mmp2)* we have observed the same opposite behaviour between the two matrices supporting our theory.

Since skeletal muscle regeneration after injury requires the activity of resident muscle stem cells, called satellite cells, we finally decided to investigate if the myogenic and adipogenic pathways were changed but also for these analysis we did not observed any statistical difference.

To summarise, our preliminary results indicate that a matrix derived from metabolically altered donor is not able to promote either a different ECM deposition or an adipose tissue increase induced by a switch of resident cells from a myogenic to an adipogenic commitment.

CONCLUSIONS AND FUTURE PERSPECTIVES

The present work has been carried out in order to explain some characteristics of the origin of a disabling pathological condition which is the sarcopenic obesity. We focusing, in particular, on two different aspects: on muscle inflammation and ECM involvement in the development of skeletal muscle loss. This is the first time in which a correlation between muscle inflammation and the analysis of serum specific muscle-derived microRNA was performed in obese patients. We observed that bariatric surgery did not improve muscle situation (indeed, no differences were noted from miRNA analysis performed on pre- and 1 year post-surgery samples). The obtained results allowed us also to observe that in metformin-treated diabetic patient a reduction in muscle inflammation was present, leading to hypothesise a further beneficial effect of this drug besides its well-known metabolic action. This study has some intrinsic limitations such as the different body districts from which biopsies were collected during surgery, and the size of the studied population. For these reasons we are carrying out a series of new experiments enrolling new patients before and after bariatric surgery in order to increase the miRNA analysis. We are also planning to investigate the role of Metformin directly on muscle stem cells isolated from muscle biopsies of human obese and healthy subjects. Using primary cells, we will be able to understand the modulation of inflammatory process following Metformin treatment directly on patient samples. In particular, isolating muscle stem cells from normoglycemic patient biopsies, treating them with different Metformin concentration and comparing inflammatory genes and muscle stem cells characteristics before and after treatment, we will be able to investigate the role of this drug on the modulation of muscle inflammation and on the ability of muscle cells recovery.

Moreover, using ob/ob mouse model we found the preliminary indications that ECM derived from a metabolically altered donors are similar to wild type ECM not only in structure and composition but also in regenerative stimuli release after *in-vivo* transplantation. Given these evidences, we are aware that only using ob/ob mice as recipient we will be able to confirm the hypothesis that obese ECM alone do not induces sarcopenic obesity since the

regeneration stimuli from the recipient side might be more specific and powerful rather than those from donor ECM.

BIBLIOGRAPHY

1. Pedersen, B.K. and M.A. Febbraio, *Muscles, exercise and obesity: skeletal muscle as a secretory organ.* Nat Rev Endocrinol, 2012. **8**(8): p. 457-65.
2. de Rezende Pinto, W.B., P.V. de Souza, and A.S. Oliveira, *Normal muscle structure, growth, development, and regeneration.* Curr Rev Musculoskelet Med, 2015. **8**(2): p. 176-81.
3. Frontera, W.R. and J. Ochala, *Skeletal muscle: a brief review of structure and function.* Calcif Tissue Int, 2015. **96**(3): p. 183-95.
4. Verfaillie, C.M., M.F. Pera, and P.M. Lansdorp, *Stem cells: hype and reality.* Hematology Am Soc Hematol Educ Program, 2002: p. 369-91.
5. Medvedev, S.P., A.I. Shevchenko, and S.M. Zakian, *Molecular basis of Mammalian embryonic stem cell pluripotency and self-renewal.* Acta Naturae, 2010. **2**(3): p. 30-46.
6. Wobus, A.M. and K.R. Boheler, *Embryonic stem cells: Prospects for developmental biology and cell therapy.* Physiological Reviews, 2005. **85**(2): p. 635-678.
7. Pappa, K.I. and N.P. Anagnou, *Novel sources of fetal stem cells: where do they fit on the developmental continuum?* Regen Med, 2009. **4**(3): p. 423-33.
8. Pessina, A. and L. Gribaldo, *The key role of adult stem cells: therapeutic perspectives.* Curr Med Res Opin, 2006. **22**(11): p. 2287-300.
9. Yin, H., F. Price, and M.A. Rudnicki, *Satellite cells and the muscle stem cell niche.* Physiological Reviews, 2013. **93**(1): p. 23-67.
10. Ceafalan, L.C., B.O. Popescu, and M.E. Hinescu, *Cellular players in skeletal muscle regeneration.* Biomed Res Int, 2014. **2014**: p. 957014.
11. Boldrin, L. and J.E. Morgan, *Human satellite cells: identification on human muscle fibres.* PLoS Curr, 2011. **3**: p. RRN1294.
12. Bentzinger, C.F., et al., *Cellular dynamics in the muscle satellite cell niche.* EMBO Rep, 2013. **14**(12): p. 1062-72.
13. Spradling, A., D. Drummond-Barbosa, and T. Kai, *Stem cells find their niche.* Nature, 2001. **414**(6859): p. 98-104.
14. Dayanidhi, S. and R.L. Lieber, *Skeletal muscle satellite cells: mediators of muscle growth during development and implications for developmental disorders.* Muscle Nerve, 2014. **50**(5): p. 723-32.
15. Wang, Y.X. and M.A. Rudnicki, *Satellite cells, the engines of muscle repair.* Nat Rev Mol Cell Biol, 2012. **13**(2): p. 127-33.
16. Kuang, S., et al., *Asymmetric self-renewal and commitment of satellite stem cells in muscle.* Cell, 2007. **129**(5): p. 999-1010.
17. Charge, S.B. and M.A. Rudnicki, *Cellular and molecular regulation of muscle regeneration.* Physiological Reviews, 2004. **84**(1): p. 209-38.
18. Ha, M. and V.N. Kim, *Regulation of microRNA biogenesis.* Nat Rev Mol Cell Biol, 2014. **15**(8): p. 509-24.
19. Dong, H., et al., *MicroRNA: Function, Detection, and Bioanalysis.* Chem Rev, 2013. **113**(8): p. 6207-33.
20. Chalfie, M., H.R. Horvitz, and J.E. Sulston, *Mutations that lead to reiterations in the cell lineages of C. elegans.* Cell, 1981. **24**(1): p. 59-69.
21. Afonso-Grunz, F. and S. Muller, *Principles of miRNA-mRNA interactions: beyond sequence complementarity.* Cell Mol Life Sci, 2015. **72**(16): p. 3127-41.
22. Mitchelson, K.R. and W.Y. Qin, *Roles of the canonical myomiRs miR-1, -133 and -206 in cell development and disease.* World J Biol Chem, 2015. **6**(3): p. 162-208.
23. Winbanks, C.E., et al., *MicroRNAs differentially regulated in cardiac and skeletal muscle in health and disease: potential drug targets?* Clin Exp Pharmacol Physiol, 2014. **41**(9): p. 727-37.

24. Horak, M., J. Novak, and J. Bienertova-Vasku, *Muscle-specific microRNAs in skeletal muscle development.* Dev Biol, 2016. **410**(1): p. 1-13.
25. Liu, W., et al., *miR-133a regulates adipocyte browning in vivo.* PLoS Genet, 2013. **9**(7): p. e1003626.
26. Chen, X., et al., *Characterization of microRNAs in serum: a novel class of biomarkers for diagnosis of cancer and other diseases.* Cell Res, 2008. **18**(10): p. 997-1006.
27. Koutsoulidou, A., et al., *Elevated Muscle-Specific miRNAs in Serum of Myotonic Dystrophy Patients Relate to Muscle Disease Progress.* PLoS One, 2015. **10**(4): p. e0125341.
28. Li, X., et al., *Circulating Muscle-specific miRNAs in Duchenne Muscular Dystrophy Patients.* Mol Ther Nucleic Acids, 2014. **3**: p. e177.
29. Theocharis, A.D., et al., *Extracellular matrix structure.* Adv Drug Deliv Rev, 2016. **97**: p. 4-27.
30. Frantz, C., K.M. Stewart, and V.M. Weaver, *The extracellular matrix at a glance.* J Cell Sci, 2010. **123**(Pt 24): p. 4195-200.
31. Bonnans, C., J. Chou, and Z. Werb, *Remodelling the extracellular matrix in development and disease.* Nat Rev Mol Cell Biol, 2014. **15**(12): p. 786-801.
32. Kular, J.K., S. Basu, and R.I. Sharma, *The extracellular matrix: Structure, composition, age-related differences, tools for analysis and applications for tissue engineering.* J Tissue Eng, 2014. **5**: p. 2041731414557112.
33. Hoshiba, T., et al., *Decellularized Extracellular Matrix as an In Vitro Model to Study the Comprehensive Roles of the ECM in Stem Cell Differentiation.* Stem Cells Int, 2016. **2016**: p. 6397820.
34. Tam, C.S., et al., *The effects of high-fat feeding on physical function and skeletal muscle extracellular matrix.* Nutr Diabetes, 2015. **5**: p. e187.
35. Toledo, F.G., et al., *Effects of physical activity and weight loss on skeletal muscle mitochondria and relationship with glucose control in type 2 diabetes.* Diabetes, 2007. **56**(8): p. 2142-7.
36. Grogan, B.F. and J.R. Hsu, *Volumetric muscle loss.* J Am Acad Orthop Surg, 2011. **19 Suppl 1**: p. S35-7.
37. Vekris, M.D., et al., *Restoration of elbow function in severe brachial plexus paralysis via muscle transfers.* Injury, 2008. **39 Suppl 3**: p. S15-22.
38. Terzis, J.K. and V.K. Kostopoulos, *Free muscle transfer in posttraumatic plexopathies: part 1: the shoulder.* Ann Plast Surg, 2010. **65**(3): p. 312-7.
39. Terzis, J.K. and V.K. Kostopoulos, *Free Muscle Transfer in Posttraumatic Plexopathies Part II: The Elbow.* Hand (N Y), 2010. **5**(2): p. 160-70.
40. Grasman, J.M., et al., *Rapid release of growth factors regenerates force output in volumetric muscle loss injuries.* Biomaterials, 2015. **72**: p. 49-60.
41. Corona, B.T., et al., *The promotion of a functional fibrosis in skeletal muscle with volumetric muscle loss injury following the transplantation of muscle-ECM.* Biomaterials, 2013. **34**(13): p. 3324-35.
42. Darabi, R., et al., *Assessment of the myogenic stem cell compartment following transplantation of Pax3/Pax7-induced embryonic stem cell-derived progenitors.* Stem Cells, 2011. **29**(5): p. 777-90.
43. De Bari, C., et al., *Skeletal muscle repair by adult human mesenchymal stem cells from synovial membrane.* J Cell Biol, 2003. **160**(6): p. 909-18.
44. Rossi, C.A., et al., *In vivo tissue engineering of functional skeletal muscle by freshly isolated satellite cells embedded in a photopolymerizable hydrogel.* FASEB J, 2011. **25**(7): p. 2296-304.

45. DiMario, J.X. and F.E. Stockdale, *Differences in the developmental fate of cultured and noncultured myoblasts when transplanted into embryonic limbs.* Exp Cell Res, 1995. **216**(2): p. 431-42.
46. Langer, R. and J.P. Vacanti, *Tissue engineering.* Science, 1993. **260**(5110): p. 920-6.
47. Badylak, S.F., D. Taylor, and K. Uygun, *Whole-organ tissue engineering: decellularization and recellularization of three-dimensional matrix scaffolds.* Annu Rev Biomed Eng, 2011. **13**: p. 27-53.
48. Hussein, K.H., et al., *Biocompatibility evaluation of tissue-engineered decellularized scaffolds for biomedical application.* Mater Sci Eng C Mater Biol Appl, 2016. **67**: p. 766-78.
49. Keane, T.J., I.T. Swinehart, and S.F. Badylak, *Methods of tissue decellularization used for preparation of biologic scaffolds and in vivo relevance.* Methods, 2015. **84**: p. 25-34.
50. Fu, R.H., et al., *Decellularization and recellularization technologies in tissue engineering.* Cell Transplant, 2014. **23**(4-5): p. 621-30.
51. Gilbert, T.W., T.L. Sellaro, and S.F. Badylak, *Decellularization of tissues and organs.* Biomaterials, 2006. **27**(19): p. 3675-83.
52. Ott, H.C., et al., *Perfusion-decellularized matrix: using nature's platform to engineer a bioartificial heart.* Nat Med, 2008. **14**(2): p. 213-21.
53. Petersen, T.H., et al., *Tissue-engineered lungs for in vivo implantation.* Science, 2010. **329**(5991): p. 538-41.
54. Uygun, B.E., et al., *Organ reengineering through development of a transplantable recellularized liver graft using decellularized liver matrix.* Nat Med, 2010. **16**(7): p. 814-20.
55. Liu, C.X., et al., *[Preparation of whole-kidney acellular matrix in rats by perfusion].* Nan Fang Yi Ke Da Xue Xue Bao, 2009. **29**(5): p. 979-82.
56. Gillies, A.R., et al., *Method for decellularizing skeletal muscle without detergents or proteolytic enzymes.* Tissue Eng Part C Methods, 2011. **17**(4): p. 383-9.
57. Meyer, S.R., et al., *Comparison of aortic valve allograft decellularization techniques in the rat.* J Biomed Mater Res A, 2006. **79**(2): p. 254-62.
58. Lehr, E.J., et al., *Decellularization reduces immunogenicity of sheep pulmonary artery vascular patches.* J Thorac Cardiovasc Surg, 2011. **141**(4): p. 1056-62.
59. Baiguera, S., et al., *Tissue engineered human tracheas for in vivo implantation.* Biomaterials, 2010. **31**(34): p. 8931-8.
60. Yang, B., et al., *Development of a porcine bladder acellular matrix with well-preserved extracellular bioactive factors for tissue engineering.* Tissue Eng Part C Methods, 2010. **16**(5): p. 1201-11.
61. Crapo, P.M., T.W. Gilbert, and S.F. Badylak, *An overview of tissue and whole organ decellularization processes.* Biomaterials, 2011. **32**(12): p. 3233-43.
62. Parmaksiz, M., et al., *Clinical applications of decellularized extracellular matrices for tissue engineering and regenerative medicine.* Biomed Mater, 2016. **11**(2): p. 022003.
63. Mizuno, H., M. Tobita, and A.C. Uysal, *Concise review: Adipose-derived stem cells as a novel tool for future regenerative medicine.* Stem Cells, 2012. **30**(5): p. 804-10.
64. Berry, D.C., et al., *The developmental origins of adipose tissue.* Development, 2013. **140**(19): p. 3939-49.
65. Hassan, M., N. Latif, and M. Yacoub, *Adipose tissue: friend or foe?* Nat Rev Cardiol, 2012. **9**(12): p. 689-702.
66. Kusminski, C.M., P.E. Bickel, and P.E. Scherer, *Targeting adipose tissue in the treatment of obesity-associated diabetes.* Nat Rev Drug Discov, 2016.

67. Cristancho, A.G. and M.A. Lazar, *Forming functional fat: a growing understanding of adipocyte differentiation.* Nat Rev Mol Cell Biol, 2011. **12**(11): p. 722-34.
68. Seale, P., et al., *PRDM16 controls a brown fat/skeletal muscle switch.* Nature, 2008. **454**(7207): p. 961-7.
69. Wu, J., et al., *Beige adipocytes are a distinct type of thermogenic fat cell in mouse and human.* Cell, 2012. **150**(2): p. 366-76.
70. Spiegelman, B.M. and J.S. Flier, *Obesity and the regulation of energy balance.* Cell, 2001. **104**(4): p. 531-43.
71. Caballero, B., *The global epidemic of obesity: an overview.* Epidemiol Rev, 2007. **29**: p. 1-5.
72. Nishtar, S., P. Gluckman, and T. Armstrong, *Ending childhood obesity: a time for action.* Lancet, 2016. **387**(10021): p. 825-7.
73. Gesta, S., et al., *Evidence for a role of developmental genes in the origin of obesity and body fat distribution.* Proc Natl Acad Sci U S A, 2006. **103**(17): p. 6676-81.
74. Grundy, S.M., et al., *Definition of metabolic syndrome: Report of the National Heart, Lung, and Blood Institute/American Heart Association conference on scientific issues related to definition.* Circulation, 2004. **109**(3): p. 433-8.
75. O'Neill, S. and L. O'Driscoll, *Metabolic syndrome: a closer look at the growing epidemic and its associated pathologies.* Obes Rev, 2015. **16**(1): p. 1-12.
76. Mingrone, G., et al., *Bariatric-metabolic surgery versus conventional medical treatment in obese patients with type 2 diabetes: 5 year follow-up of an open-label, single-centre, randomised controlled trial.* Lancet, 2015. **386**(9997): p. 964-73.
77. Mechanick, J.I., et al., *American Association of Clinical Endocrinologists, The Obesity Society, and American Society for Metabolic & Bariatric Surgery medical guidelines for clinical practice for the perioperative nutritional, metabolic, and nonsurgical support of the bariatric surgery patient.* Obesity (Silver Spring), 2009. **17 Suppl 1**: p. S1-70, v.
78. Lee, W.J., et al., *Metabolic Surgery for Diabetes Treatment: Sleeve Gastrectomy or Gastric Bypass?* World J Surg, 2016.
79. Creange, C., et al., *The safety of laparoscopic sleeve gastrectomy among diabetic patients.* Surg Endosc, 2016.
80. Addison, O., et al., *Intermuscular Fat: A Review of the Consequences and Causes.* Int J Endocrinol, 2014. **2014**: p. 309570.
81. Vettor, R., et al., *The origin of intermuscular adipose tissue and its pathophysiological implications.* Am J Physiol Endocrinol Metab, 2009. **297**(5): p. E987-98.
82. Joe, A.W., et al., *Muscle injury activates resident fibro/adipogenic progenitors that facilitate myogenesis.* Nat Cell Biol, 2010. **12**(2): p. 153-63.
83. Farup, J., et al., *Interactions between muscle stem cells, mesenchymal-derived cells and immune cells in muscle homeostasis, regeneration and disease.* Cell Death Dis, 2015. **6**: p. e1830.
84. Laurens, C. and C. Moro, *Intramyocellular fat storage in metabolic diseases.* Horm Mol Biol Clin Investig, 2016. **26**(1): p. 43-52.
85. Xaymardan, M., J.R. Gibbins, and H. Zoellner, *Adipogenic healing in adult mice by implantation of hollow devices in muscle.* Anat Rec, 2002. **267**(1): p. 28-36.
86. van Loon, L.J. and B.H. Goodpaster, *Increased intramuscular lipid storage in the insulin-resistant and endurance-trained state.* Pflugers Arch, 2006. **451**(5): p. 606-16.

87. Gopinath, S.D. and T.A. Rando, *Stem cell review series: aging of the skeletal muscle stem cell niche.* Aging Cell, 2008. **7**(4): p. 590-8.
88. Schultz, M.B. and D.A. Sinclair, *When stem cells grow old: phenotypes and mechanisms of stem cell aging.* Development, 2016. **143**(1): p. 3-14.
89. Garcia-Prat, L. and P. Munoz-Canoves, *Aging, metabolism and stem cells: Spotlight on muscle stem cells.* Mol Cell Endocrinol, 2016.
90. Rosenberg, I.H., *Sarcopenia: origins and clinical relevance.* J Nutr, 1997. **127**(5 Suppl): p. 990S-991S.
91. Cruz-Jentoft, A.J., et al., *Sarcopenia: European consensus on definition and diagnosis: Report of the European Working Group on Sarcopenia in Older People.* Age Ageing, 2010. **39**(4): p. 412-23.
92. Molino, S., et al., *Sarcopenic Obesity: An Appraisal of the Current Status of Knowledge and Management in Elderly People.* J Nutr Health Aging, 2016. **20**(7): p. 780-8.
93. Kalinkovich, A. and G. Livshits, *Sarcopenic obesity or obese sarcopenia: a cross talk between age-associated adipose tissue and skeletal muscle inflammation as a main mechanism of the pathogenesis.* Ageing Res Rev, 2016.
94. Dominguez, L.J. and M. Barbagallo, *The biology of the metabolic syndrome and aging.* Curr Opin Clin Nutr Metab Care, 2016. **19**(1): p. 5-11.
95. Kalyani, R.R., M. Corriere, and L. Ferrucci, *Age-related and disease-related muscle loss: the effect of diabetes, obesity, and other diseases.* Lancet Diabetes Endocrinol, 2014. **2**(10): p. 819-29.
96. Pillon, N.J., et al., *Cross-talk between skeletal muscle and immune cells: muscle-derived mediators and metabolic implications.* Am J Physiol Endocrinol Metab, 2013. **304**(5): p. E453-65.
97. Erskine, R.M., et al., *The individual and combined effects of obesity- and ageing-induced systemic inflammation on human skeletal muscle properties.* Int J Obes (Lond), 2016.
98. Costamagna, D., et al., *Role of Inflammation in Muscle Homeostasis and Myogenesis.* Mediators Inflamm, 2015. **2015**: p. 805172.
99. Sadtler, K., et al., *Developing a pro-regenerative biomaterial scaffold microenvironment requires T helper 2 cells.* Science, 2016. **352**(6283): p. 366-70.
100. Saini, J., et al., *Regenerative function of immune system: Modulation of muscle stem cells.* Ageing Res Rev, 2016. **27**: p. 67-76.
101. Osborn, O. and J.M. Olefsky, *The cellular and signaling networks linking the immune system and metabolism in disease.* Nat Med, 2012. **18**(3): p. 363-74.
102. Dunn, C.J. and D.H. Peters, *Metformin. A review of its pharmacological properties and therapeutic use in non-insulin-dependent diabetes mellitus.* Drugs, 1995. **49**(5): p. 721-49.
103. Saisho, Y., *Metformin and Inflammation: Its Potential Beyond Glucose-lowering Effect.* Endocr Metab Immune Disord Drug Targets, 2015. **15**(3): p. 196-205.
104. Wang, J., et al., *Metformin activates an atypical PKC-CBP pathway to promote neurogenesis and enhance spatial memory formation.* Cell Stem Cell, 2012. **11**(1): p. 23-35.
105. Sasaki, H., et al., *Metformin prevents progression of heart failure in dogs: role of AMP-activated protein kinase.* Circulation, 2009. **119**(19): p. 2568-77.
106. Evans, J.M., et al., *Metformin and reduced risk of cancer in diabetic patients.* BMJ, 2005. **330**(7503): p. 1304-5.
107. Martin-Montalvo, A., et al., *Metformin improves healthspan and lifespan in mice.* Nat Commun, 2013. **4**: p. 2192.

108. Turban, S., et al., *Defining the contribution of AMP-activated protein kinase (AMPK) and protein kinase C (PKC) in regulation of glucose uptake by metformin in skeletal muscle cells.* J Biol Chem, 2012. **287**(24): p. 20088-99.
109. Musi, N., et al., *Metformin increases AMP-activated protein kinase activity in skeletal muscle of subjects with type 2 diabetes.* Diabetes, 2002. **51**(7): p. 2074-81.
110. Park, C.S., et al., *Metformin reduces airway inflammation and remodeling via activation of AMP-activated protein kinase.* Biochem Pharmacol, 2012. **84**(12): p. 1660-70.
111. Kemp, J.G., et al., *Morphological and biochemical alterations of skeletal muscles from the genetically obese (ob/ob) mouse.* Int J Obes (Lond), 2009. **33**(8): p. 831-41.
112. Piccoli, M., et al., *Improvement of diaphragmatic performance through orthotopic application of decellularized extracellular matrix patch.* Biomaterials, 2016. **74**: p. 245-55.
113. Hruby, A. and F.B. Hu, *The Epidemiology of Obesity: A Big Picture.* Pharmacoeconomics, 2015. **33**(7): p. 673-89.
114. Kim, S.A. and H.C. Choi, *Metformin inhibits inflammatory response via AMPK-PTEN pathway in vascular smooth muscle cells.* Biochem Biophys Res Commun, 2012. **425**(4): p. 866-72.
115. Alvarez, M.M., et al., *Delivery strategies to control inflammatory response: Modulating M1-M2 polarization in tissue engineering applications.* J Control Release, 2016. **240**: p. 349-363.
116. Klopfleisch, R., *Macrophage reaction against biomaterials in the mouse model - Phenotypes, functions and markers.* Acta Biomater, 2016. **43**: p. 3-13.